The Mathematical Analysis of Biological Aggregation and Dispersal: Progress, Problems and Perspectives

Hans G. Othmer and Chuan Xue

Abstract Motile organisms alter their movement in response to signals in their environment for a variety of reasons, such as to find food or mates or to escape danger. In populations of individuals this often this leads to large-scale pattern formation in the form of coherent movement or localized aggregates of individuals, and an important question is how the individual-level decisions are translated into population-level behavior. Mathematical models are frequently developed for a population-level description, and while these are often phenomenological, it is important to understand how individual-level properties can be correctly embedded in the population-level models. We discuss several classes of models that are used to describe individual movement and indicate how they can be translated into population-level models.

1 Introduction

The central topic of this chapter is the process of aggregation of biological organisms, which occurs in systems that range in scale from single-celled organisms such as the bacterium *E. coli*, to flocks of birds, schools of fish, and herds of ungulates. Aggregation is a broad term, which we use to mean a self-induced spatial localization of motile individuals that results from direct or indirect communication between them and produces a local density of individuals higher than would be observed under random motion. Depending on the organisms involved, more

H.G. Othmer (✉)
School of Mathematics and Digital Technology Center, University of Minnesota, Minneapolis, MN 55455, USA
e-mail: othmer@math.umn.edu

C. Xue
Mathematical Biosciences Institute, Ohio State University, Columbus, OH 43210, USA
e-mail: cxue@mbi.osu.edu

M.A. Lewis et al. (eds.), *Dispersal, Individual Movement and Spatial Ecology*, Lecture Notes in Mathematics 2071, DOI 10.1007/978-3-642-35497-7_4,

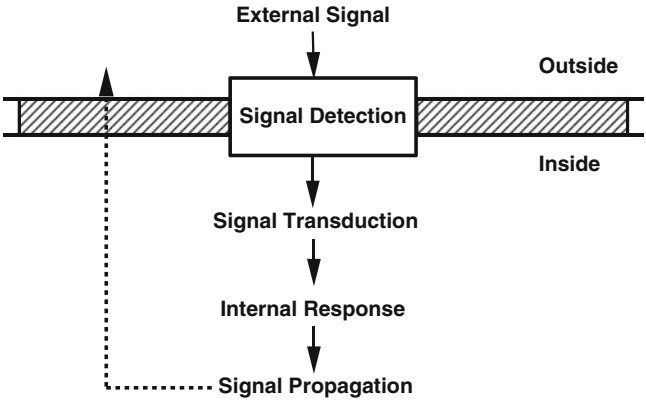

Fig. 1 The general steps involved in generating the response to an external signal

specific terms may be used: swarming in insects, flocking in birds, schooling in fishes and herding in mammals—but all refer to the same underlying process. In some aggregates there is large scale organization, such as alignment in fish schools, which undoubtedly involves at least nearest-neighbor interactions, whereas in other aggregates, such as the bacterial aggregates discussed later, there is no coherence to the motion even though there may be indirect interaction between individuals via the external medium. Whatever the scale or type of aggregation, locomotion—which we define to be self-induced movement that results from active forces generated by the individual—is an essential process in aggregation, but of course it also plays a role in numerous other contexts, including searching for food, mates or shelter. For example cell locomotion, either individually or collectively as tissues, is essential for early development, angiogenesis, tissue regeneration, the immune response, and wound healing in multicellular organisms, and plays a very deleterious role in cancer metastasis in humans. Directed locomotion, as opposed to random wandering, usually involves several steps (i) the detection and transduction of external signals, be they visual, chemical, mechanical, or of other types, (ii) integration of the signals into an internal signal, (iii) the control of the internal neural, biochemical and mechanical responses that lead to force generation and directed movement, and (iv) perhaps relay of the signal. A schematic of the sub-processes involved is shown in Fig. 1.

A detailed description of locomotion of higher organisms such as birds or fishes is extremely complex, and simpler descriptions are used for understanding aggregation. A starting point is to treat individuals as points and attempt to understand the collective behavior of an aggregate based on postulated interactions between individuals or between individuals and an external field, either imposed or generated by the population. In this framework the problem is mathematically similar to the study of interacting molecular species, and techniques established in that context can be carried over to biological problems. Because single cells are the simplest systems capable of self-locomotion, the description of cellular motion can

be more complete in models of aggregation, but the principles that emerge from the analysis of cellular motion apply at higher levels as well. Thus several concrete examples of cell-level aggregation will be described in detail later.

Many single-celled organisms use flagella or cilia to swim, and the best studied example of this is *E. coli*. As we show later, much can be learned about 'run-and-tumble' organisms such as *E. coli* without a detailed description of the mechanical forces, but in eukaryotes forces play a more central role. There are two basic modes of movement used by eukaryotic cells that lack cilia or flagella—mesenchymal and amoeboid [10]. The former, which can be characterized as 'crawling' in fibroblasts or 'gliding' in keratocytes, involves the extension of finger-like filopodia or pseudopodia and/or broad flat lamellipodia, whose protrusion is driven by actin polymerization at the leading edge. This mode dominates in cells such as fibroblasts when moving on a 2D substrate. In the amoeboid mode, which does not rely on strong adhesion, cells are more rounded and employ shape changes to move—in effect 'jostling through the crowd' or 'swimming'. Recent experiments have shown that numerous eukaryotic cell types display enormous plasticity in locomotion in that they sense the mechanical properties of their environment and adjust the balance between the modes accordingly by altering the balance between parallel signal transduction pathways [85]. Thus pure crawling and pure swimming are the extremes on a continuum of locomotion strategies for eukaryotic cells, but many cells can sense their environment and use the most efficient strategy in a given context. Significant progress has been made in going beyond the point particle description in such systems (cf. [90] and references therein).

Some basic questions that arise in studying aggregation, either from the experimental or mathematical standpoint, are as follows.

- At what level of detail must individuals be described to explain the observed phenomena?
- What is the coarsest or highest-level description of the forces involved that suffices?
- What is the nature of the signal that is used to initiate aggregation? Is the signal externally-imposed, as for example, when bacteria move up the gradient of a desirable substance, is the signal relayed from individual to individual, and what is the range of the signal?
- What determines the size of an aggregate and how does it depend on the nature and range of the signal?
- When aggregates move coherently, by which we mean they locally adjust their speed and direction to those of their neighbors, the latter perhaps weighted in decreasing importance with distance, what is the time scale on which coherence is achieved beginning from an incoherent state, and how does the type of signal and its range affect this time.

There is a huge literature on the subject of aggregation, orientation and alignment, and other chapters in this volume will cover other aspects (see the chapters by Hillen and Painter and by Franz and Erban). Recent papers that discuss some of the topics treated herein are given in [6, 14, 21, 67, 94, 95]. Classic texts related

to the topics herein include [9, 69]. We have two main objectives here: (i) to summarize some of the recent work on the derivation of macroscopic equations such as the Patlak-Keller-Segel chemotaxis equations from individual-based descriptions, and (ii) to illustrate the use of the macroscopic equations that result in cellular aggregation.

The classical taxis problem began with phenomenological equations in which a biased drift term was added to a diffusion equation to describe the movement of individuals in response to an imposed or self-generated signal [52], although a more fundamental approach along the lines described later was initiated earlier by Patlak [80], and the resulting taxis equation is called the PKS equation. To describe it more precisely, let $\Omega \subset R^n$ be a compact domain with smooth boundary, let n be the 'particle' density, and let S be the 'signal' density. The first of the following pair is the PKS equation, and the second describes the self-generated signal field, when applicable.

$$n_t = \nabla \cdot (\nabla n - n\nabla \Phi(S)) = \nabla \cdot (\nabla n - n\chi(S)\nabla S), \tag{1}$$

$$S_t = D\Delta S + f(n, S). \tag{2}$$

The first rigorous derivation of the coupled equations beginning with an interacting particle system is due to Stevens [89]. A review of the major developments from 1970 to about 2003 can be found in [45], and a 'user's guide' to these and other taxis equations can be found in [42]. The quantity $\chi \equiv \Phi_S(n, S, x, \dots)$ is called the chemotactic sensitivity, and $\mathbf{u}_c \equiv \chi(S)\nabla S$ is called the chemotactic velocity, and the fundamental problem we address is how knowledge of the internal dynamics governing signal transduction and response is reflected in these quantities. We develop the machinery for addressing this and describe some success for simple organisms such as *E. coli*, and partial success for eukaryotic cells.

2 An Overview of Population-Level Descriptions

2.1 A Summary of the Levels of Description

We begin by summarizing classical approaches to the transition from equations of motion for individuals to population level distribution functions. The material in this section is standard and widely-discussed, but it is useful to remind the reader of some of the underlying assumptions. To understand the broad picture before delving into the details, we regard the particles or individuals as structureless, but we admit the possibility that they can exert forces and allow for external forces as well. We first consider point particles, and thus describe their motion by Newton's law. For later purposes we include an evolution equation for the internal state of the particles, but at present we do not include coupling of the latter to the movement. The general case of forcing on both position and velocity leads to the differential equations

$$\mathrm{d}\mathbf{x}_i = \mathbf{v}_i\,\mathrm{dt} + \mathrm{d}\mathbf{X}_i, \tag{3}$$

$$m_i\mathrm{d}\mathbf{v}_i = \mathbf{F}_i\,\mathrm{dt} + \mathrm{d}\mathbf{V}_i, \tag{4}$$

$$\frac{dy}{dt} = G(\mathbf{x}, \mathbf{v}, y, t). \tag{5}$$

Here $(\mathbf{x}, \mathbf{v}) \in R^n, n = 1, 2, 3$ are the positions and velocities, and $y \in R^s$ characterizes the internal state. If the imposed forces $\mathbf{X}$ and $\mathbf{V}$ are deterministic forces they can be written as $d\mathbf{X}_i = X_i\,dt$, and similarly for $d\mathbf{V}$, and (3) and (4) are the standard Newton equations for particles. When $\mathbf{X}$ and $\mathbf{V}$ are random forces these are stochastic differential equations, the integral forms of which are interpreted in the Ito sense [4, 13].

The two major types of random forcing processes that are widely used are Brownian motion and compound Poisson processes. Both Brownian motion and the Poisson process are examples of a more general class of random processes called Lévy processes [2, 86], which are stochastic processes that have independent, stationary increments, are stochastically continuous, i.e., for any $\epsilon > 0$, $\Pr\{|X_{t+s} - X_s| > \epsilon\} \to 0$ as $t \to 0$, and have sample paths that are right-continuous and have left limits. Brownian motion and Poisson processes differ in that the former have continuous sample paths whereas Poisson processes have discontinuities at the jump. Lévy processes with fat-tailed distributions will arise in Sect. 3.4 in the context of anomalous diffusion.

The formal differentials that appear in (3) and (4) are assumed to be white noise, which is a wide-sense stationary random process in which the component functions $d\mathbf{X}_i$ have zero mean and are uncorrelated, i.e.,

$$\langle \mathrm{d}\mathbf{X}_i(t) \rangle = 0, \tag{6}$$

$$\langle \mathrm{d}\mathbf{X}_i(t_1), \mathrm{d}\mathbf{X}_i(t_2) \rangle = \sigma^2 \delta(t_1 - t_2). \tag{7}$$

Gaussian white noise is the generalized derivative of a single-variable Wiener process, i.e., of Brownian motion [4, 36].

As used here, a Poisson forcing function is a compound Poisson process, which can be thought of as a train of jumps distributed in time according to a Poisson law. Thus

$$\mathbf{X}_i(t) = \sum_{k=1}^{N(t)} Y_k H(t - t_k), \tag{8}$$

where the amplitudes Y_k are independent random variables, H is the step function, and $N(t)$ is a homogeneous Poisson counting process with parameter λ that counts the number of jumps in $[0, t]$, assuming that $N(0) = 0$ with certainty. A generalization of this allows coupling between the amplitudes of the impulses and their temporal occurrence, and can be defined by a random measure $M(dt, dY)$ that gives the number of jumps in $((t, t + dt) \times (y, y + dy))$. The derivative of the forcing, which is called Poisson white noise, is thus a train of impulses that arrive at the jump times of the underlying Poisson process.

$$d\mathbf{X}_i(t) = \sum_{k=1}^{N(t)} Y_k \delta(t - t_k), \tag{9}$$

Later we allow the Poisson parameter to depend on external fields or on the internal state of individuals.

The simplest problem arises when there are no inter-particle interactions, and the forces stem from interactions with the environment. One example is the original Einstein model of a heavy particle in a bath that receives Gaussian-distributed momentum impulses from the surrounding bath [27]. In Einstein's formulation this leads to the diffusion equation for the position of the particle, and the probability to find a walker at $x \in R$, having started at the origin at $t = 0$, is

$$P(x,t) = \frac{1}{\sqrt{4\pi Dt}}\, e^{-x^2/4Dt}, \tag{10}$$

for $(x,t) \in R \times R^+$. In the next section we discuss descriptions that account for both velocity and position.

When there are impulsive forces, rather than Gaussian forces on the position in (3) we obtain the familiar random walk, in which there are instantaneous changes in position at random times. These are called space-jump processes [73], and later we show that the probability density for such a process satisfies the renewal equation

$$P(\mathbf{x},t|0) = \hat{\Phi}(t)\delta(\mathbf{x}) + \int_0^t \int_{R^n} \phi(t-\tau) T(\mathbf{x},\mathbf{y}) P(\mathbf{y},\tau|0)\, d\mathbf{y}\, d\tau. \tag{11}$$

Here $P(\mathbf{x},t|0)$ is the conditional probability that a walker who begins at the origin at time zero is in the interval $(\mathbf{x}, \mathbf{x} + d\mathbf{x})$ at time t, $\phi(t)$ is the density for the waiting time distribution, $\hat{\Phi}(t)$ is the complementary cumulative distribution function associated with $\phi(t)$, and $T(\mathbf{x},\mathbf{y})$ is the redistribution kernel for the jump process. In Sect. 3.2 we show that this also leads to diffusion equations in certain limits, which reflects the fact that under mild conditions on the distribution of jump sizes the compound Poisson process approaches Brownian motion in the limit $\lambda \to \infty$.

If we admit impulsive forces on the velocity in (4) then we arrive at the second major type of jump-driven movement, which is called a velocity jump process [73]. As described in detail later, the motion consists of a sequence of "runs" separated by re-orientations, during which a new velocity is chosen instantaneously. If we assume that the velocity changes are the result of a Poisson process of intensity λ, then in the absence of other forces we show later that we obtain the evolution equation

$$\frac{\partial p}{\partial t} + \nabla_{\mathbf{x}} \cdot \mathbf{v} p + \nabla_{\mathbf{v}} \cdot \mathbf{F} p = -\lambda p + \lambda \int T(\mathbf{v},\mathbf{v}') p(\mathbf{x},\mathbf{v}',t)\, d\mathbf{v}'. \tag{12}$$

A similar equation to describe the random movement of bacteria was first derived by Stroock [91].

2.2 The Fokker-Planck and Smoluchowski Equations

A generalization of the Einstein description of Brownian motion involves both velocity-dependent interaction of the particle with a fluid environment, and diffusion in velocity space. This is based on (3) and (4), in which we assume that the forcing on position is zero, the random forcing on velocity is Gaussian white noise, and we allow velocity-dependent frictional forces. In the standard notation of statistical physics, we write

$$\mathrm{d}\mathbf{x}_i = \mathbf{v}_i \mathrm{d}t, \tag{13}$$

$$m\mathrm{d}\mathbf{v} = -m\zeta\mathbf{v}\mathrm{d}t + \mathbf{F}\mathrm{d}t + \sqrt{2\zeta m k_B T}\, dW(t), \tag{14}$$

where ζ is the friction coefficient, k_B is Boltzmann's constant and T is the temperature. This description is predicated on the assumption that the fluid particles are much lighter than the Brownian particle, and as a result, that the fluid motion relaxes on a much shorter time scale than the motion of the particle. Thus the hydrodynamic forces appear both via the deterministic friction force and the random forces, which are assumed to be Gaussian. If the assumption on the relaxation time of the fluid variables is not applicable the process is no longer Markovian, and a non-Markovian generalization of (14) has been derived [11].

The stochastic differential equations are equivalent, under the Gaussian assumption, to a partial differential equation for the conditional probability density $p(\mathbf{x}, \mathbf{v}, t|\mathbf{x}', \mathbf{v}', t')$, namely,

$$\frac{\partial p}{\partial t} + \nabla_{\mathbf{x}} \cdot \mathbf{v} p + \nabla_{\mathbf{v}} \cdot \left(\left(-\zeta \mathbf{v} + \frac{\mathbf{F}}{m} \right) p \right) = \frac{\zeta k_B T}{m} \nabla_{\mathbf{v}} \cdot \nabla_{\mathbf{v}} p. \tag{15}$$

This is commonly called the Fokker-Planck-Kramers-Klein equation [100], or simply the Fokker-Planck equation, although the latter is used for a much broader class of equations [18, 36, 50]. This is a mixed-type equation that describes drift-diffusion in the velocity component and drift in $\mathbf{x}$ due to the external force. If the latter vanishes it reduces to pure drift-diffusion in velocity space. The equation has also been formally generalized to describe the motion of multiple Brownian particles by incorporating an integral operator on the right-hand side to account for particle-particle interactions [63].

If the friction coefficient ζ is large, one may intuitively expect that the velocity relaxes on a time scale $\mathcal{O}(\zeta^{-1})$, and then (14) reduces to an algebraic equation that can be used to replace the velocity in (13). The result is the Smoluchowski equation

$$\frac{\partial n}{\partial t} = D \nabla_{\mathbf{x}} \cdot \left(\nabla_{\mathbf{x}} n - \frac{1}{k_B T} \mathbf{F} n \right), \tag{16}$$

for the number density $n(\mathbf{x}, t) = \int p d\mathbf{v}$, where the diffusion coefficient is defined by the Einstein relation

$$D = \frac{k_B T}{\zeta}.$$

Clearly this has the form of the PKS equation (1) for a suitable choice of the force. However, the reduction as described is formal, since the full equation is a singularly-perturbed hyperbolic equation, and (16) only describes the outer solution [100]. Smoluchowski equations have been widely used in the studies of aggregation, but the limitations are frequently not appreciated. Similar issues arise in the diffusion approximation of velocity-jump processes described in Sect. 4, and we will return to them there.

2.3 *Interacting Particles, Liouville's Equation and Reduced Descriptions*

Next we suppose that there are no external forces — only inter-particle forces. Newton's second law for the system reads

$$\begin{aligned} \frac{d\mathbf{x}}{dt} &= \mathbf{v} \\ M\frac{d\mathbf{v}}{dt} &= \mathbf{F}(\mathbf{x}) \end{aligned} \tag{17}$$

where $\mathbf{x} = (\mathbf{x}_1, \mathbf{x}_2, \cdots, \mathbf{x}_N)$ is the vector of positions, $\mathbf{v} = (\mathbf{v}_1, \cdots, \mathbf{v}_N)$, $\mathbf{F} = (\mathbf{F}_1, \cdots, \mathbf{F}_N)$, and M is the diagonal matrix with $M_{ii} = m_i$. Note that we assume here that $\mathbf{F}_i$ does not depend on the velocity of any particle, nor does it depend explicitly on time. Velocity-dependence introduces dissipation and substantially changes the BBGKY hierarchy developed later. Thus there is no built-in friction-like force such as arises when an individual interacts with the background environment, nor is there a force for alignment, with the result that it may be difficult to obtain alignment of individuals for such models. This is in contrast to the force

$$\mathbf{F}_i(\mathbf{r}_{ij}) = \sum_j \phi(|\mathbf{r}_{ij}|)(\mathbf{v}_i - \mathbf{v}_j), \tag{18}$$

used in the Cucker-Smale model [22], where $\phi(s)$ is a monotone decreasing function. We assume hereafter that force between i and j depends only on their separation, i.e.,

$$\mathbf{F}_i(\mathbf{x}_j) = \mathbf{F}_i(\mathbf{r}_{ij}) \equiv \mathbf{F}(\mathbf{r}_{i1} \ldots, \mathbf{r}_{ii-1}, \mathbf{r}_{ii+1}, \ldots \mathbf{r}_{iN}),$$

where $\mathbf{r}_{ij} \equiv |\mathbf{x}_i - \mathbf{x}_j|$. Furthermore, we assume that the particles are identical, and that the forces are conservative. Then there is a potential Φ such that

$$\mathbf{F}_i(\mathbf{r}_{ij}) = -\nabla_{\mathbf{x}_i}\Phi,$$

and we assume that Φ can be written as the sum of pairwise interaction potentials

$$\Phi = \sum_{i<j}^{N} \varphi(\mathbf{r}_{ij}).$$

While (17) can be solved locally for N (in fact global solutions exist when Φ is the Newtonian potential and $N \geq 2$, as long as there are no collisions [97]), a less detailed description of the system for large N can be gotten by finding the joint probability $P_N(\mathbf{x}_1, \mathbf{x}_2, \ldots \mathbf{x}_N,\ \mathbf{v}_1, \ldots \mathbf{v}_N, t) = P_N(\mathbf{x}, \mathbf{v}, t)$ that particle i has position $\mathbf{x}_i$ and velocity $\mathbf{v}_i$. Denote the solution of (17) subject to $\mathbf{x}(0) = \mathbf{x}_o, \mathbf{v}(0) = \mathbf{v}_o$ as $(\mathbf{x}, \mathbf{v}) = (\chi(\mathbf{x}_o, \mathbf{v}_o, t), \mathscr{V}(\mathbf{x}_o, v_o, t))$, which defines a unique curve in the 6N-dimension phase space for suitable $\mathbf{F}_i$, and implies that

$$P_N(\mathbf{x}, \mathbf{v}, t) = \Pi_{i=1}^{N}\, \delta\left(\mathbf{x}_i - \chi_i(\mathbf{x}_o, \mathbf{v}_o, t)\right)\ \Pi_{i=1}^{N}\, \delta\left(\mathbf{v}_i - V_i(\mathbf{x}_o, \mathbf{v}_o, t)\right).$$

Thus if we specify an initial condition with certainty then the probability distribution at any later time is concentrated at one point. Now suppose that we run the 'experiment' many times or that we consider a large number of copies of the system. Given a distribution of initial conditions, P_N is no longer concentrated at a point or a finite number of points, but since there is no dissipation, the evolution of P_N follows from the Reynolds transport theorem [3]. Thus the N-particle distribution function evolves according to

$$\frac{\partial P_N}{\partial t} + \mathbf{v} \cdot \nabla_{\mathbf{x}} P_N + \frac{\mathbf{F}}{\mathrm{m}} \cdot \nabla_{\mathbf{v}} P_N = 0, \tag{19}$$

which is called Liouville's equation. This is formally equivalent to Newton's equations and thus equally intractable for large numbers of particles, but one can derive equations for reduced or marginal distribution functions, defined as

$$P_l(\mathbf{x}_1, \ldots \mathbf{x}_l, \mathbf{v}_1, \ldots \mathbf{v}_l, t) \equiv \int P_N(\mathbf{x}, \mathbf{v}, t) d\mathbf{x}_{l+1} \ldots d\mathbf{x}_N d\mathbf{v}_{l+1} \ldots d\mathbf{v}_N.$$

Liouville's equation can be written

$$\frac{\partial P_N}{\partial t} + \sum_{k=1}^{N} \mathbf{v}_k \cdot \nabla_{\mathbf{x}_k} P_N - \sum_{\substack{j=1 \\ i,i<j}}^{N} \frac{1}{m} \left[\frac{\partial}{\partial \mathbf{x}_i} \varphi(\mathbf{r}_{ij}) \cdot \frac{\partial}{\partial \mathbf{v}_i} + \frac{\partial}{\partial \mathbf{x}_j} \varphi(\mathbf{r}_{ij}) \cdot \frac{\partial}{\partial \mathbf{v}_j} \right] P_N = 0 \tag{20}$$

and more compactly as

$$\frac{\partial P_N}{\partial t} + \mathscr{L}_N P_N = 0. \tag{21}$$

By integrating over $N - l$ particles one obtains the evolution equation for the l-particle distribution function [16]

$$\frac{\partial f_l}{\partial t} + \mathscr{L}_\ell f_l = -\sum_{i=1}^{l} \frac{\partial}{\partial \mathbf{v}_i} \cdot \int \frac{\mathscr{F}_{i,l+1}}{m} f_{l+1}(\mathbf{x}_1, \ldots \mathbf{x}_{l+1}, \mathbf{v}_1, \ldots \mathbf{v}_{l+1}, t) d\mathbf{x}_{l+1} d\mathbf{v}_{l+1} \tag{22}$$

where

$$\mathscr{F}_{ij} \equiv -\frac{\partial \varphi(\mathbf{r}_{ij})}{\partial \mathbf{x}_i}$$

is the force between particles i and j. These equations for $l = 1, \cdots, N$ are called the BBGKY hierarchy. Clearly the system is not closed unless $l = N$, because for any $l < N$ one must know P_{l+1} to solve (22). Thus we seem once again to have come full circle; the only self-contained equation is Liouville's equation and it is equivalent to Newton's equations.

Of particular use in this context are the evolution equations for the one- and two-particle number density functions.

$$\frac{\partial P_1}{\partial t} + \mathscr{L}_1 P_1 = -\frac{\partial}{\partial \mathbf{v}_1} \cdot \int \frac{\mathscr{F}_{1,2}}{m} P_2(\mathbf{x}_1, \mathbf{x}_2, \mathbf{v}_1, \mathbf{v}_2) d\mathbf{x}_2 d\mathbf{v}_2. \tag{23}$$

$$\frac{\partial P_2}{\partial t} + \mathscr{L}_2 P_2 = -\int \left[\frac{\partial}{\partial \mathbf{v}_1} \cdot \frac{\mathscr{F}_{1,3}}{m} + \frac{\partial}{\partial \mathbf{v}_2} \cdot \frac{\mathscr{F}_{2,3}}{m} \right] P_3(\cdots) d\mathbf{x}_3 d\mathbf{v}_3 \tag{24}$$

As noted previously, when there are no collisions Liouville's equation has a smooth global solution for suitable potentials—it is the collisions that lead to Boltzmann's equation. When only binary interactions are involved, i.e., in the dilute limit, the two-particle distribution function factors and the equation for the single-particle distribution reduces to Boltzmann's equation [12]. Convergence of solutions of the BBGKY solution hierarchy to a smooth solution of a kinetic equation for a single particle distribution function is still an unresolved problem for general particle-particle interactions. A very accessible discussion of this, and in particular of the Boltzmann-Grad continuum limit $N \to \infty, \sigma^2 \to 0$ $N\sigma^2 =$ constant, is given in Cercignani et al. [17]. More complete treatments of mathematical techniques for kinetic equations are given in [16, 17, 60, 83]. Application of the BBGKY hierarchy to derive reduced descriptions for flocking problems is widely-used [15, 38], but the use of idealized kinetic models frequently fails to capture some essential characteristics of animal movement [47].

3 Simple and Reinforced Random Walks in Space

3.1 The Pearson Random Walk

Consider a random jump process on R^n in which the walker executes a sequence of jumps of negligible duration, driven by Poisson forcing $\mathbf{x}$. This is called a random walk, and the earliest analyses of these processes apparently dates to Bachelier [5] around 1900, in the context of his analysis of financial time series. However

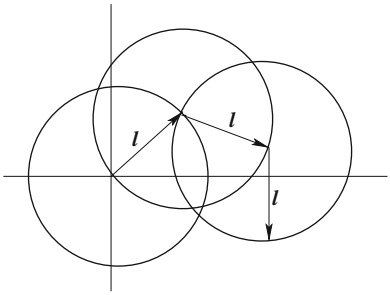

Fig. 2 Three steps in a Pearson walk of fixed step-length

the term 'random walk' was apparently coined by Pearson [81], who proposed the following problem.

A man starts from the point O and walks ℓ yards in a straight line; he then turns through any angle whatever and walks another ℓ yards in a second straight line. He repeats this process n times. I require the probability that after n stretches he is at a distance between r and $r + \delta r$ from his starting point O.

The solution to this problem had previously been obtained by Rayleigh [84] in a study of the superposition of sound waves. Later we will see that this walk fits into a more general framework that incorporates a waiting time distribution and a jump size distribution, but for now we treat the simple 2D walk shown in Fig. 2. Let $P_n(\mathbf{r})$ be the probability that a walker who begins at the origin is in the interval $(\mathbf{r}, \mathbf{r} + d\,\mathbf{r})$ at the nth step, and $T(\boldsymbol{\rho})$ be the probability of taking a step of length $|\boldsymbol{\rho}|$ in the direction $\boldsymbol{\rho}/|\boldsymbol{\rho}|$. If the steps are uncorrelated then $P_n(\mathbf{r})$ satisfies the renewal equation

$$P_{n+1}(\mathbf{r}) = \int_{R^2} T(\boldsymbol{\rho}) P_n(\mathbf{r} - \boldsymbol{\rho}) d\,\boldsymbol{\rho}. \tag{25}$$

In the Pearson walk the angular distribution is uniform on the circle of radius ℓ and thus

$$T(\boldsymbol{\rho}) = \frac{\delta(|\boldsymbol{\rho}| - \ell)}{2\pi\ell},$$

and for this kernel the probability at the $n + 1$st step is simply the average of the probabilities at the previous step over the circle of radius ℓ centered at $\mathbf{r}$. The solution of (25) is

$$P_n(\mathbf{r}) = \frac{1}{2\pi} \int_0^\infty J_0^n(k\ell) J_0(kr) k\,dk, \tag{26}$$

where $r = |\mathbf{r}|$ [7, 55], and in the limit $n \to \infty$ this reduces to

$$P_n(\mathbf{r}) \sim \frac{1}{n\pi\,\ell^2} e^{-r^2/n\,\ell^2}. \tag{27}$$

The result sought by Pearson is just $2\pi r$ times this, i.e.,

$$P_n(r) \sim \frac{2r}{n\ell^2} e^{-r^2/n\ell^2}$$

which is Rayleigh's result. In an historical coincidence, Einstein's seminal paper [27] on Brownian motion also appeared in 1905, and the parallel between (10) and (27) for the discrete Pearson walk is evident. An isotropic diffusion equation is also derived from the Pearson walk in the chapter by Hillen and Painter, using different notation.

A variation of the 2D Pearson-Rayleigh random walk in which the steps are random vectors of exponential length and uniform orientation was considered in [33]. It is shown there that imposing a constraint of a fixed total length on a walk leads to a number of interesting results. For instance, by taking exactly three steps the probability distribution is uniform in the disc of radius l, while for fewer steps the distribution is concentrated near the boundary and for more it is concentrated near the origin.

3.2 The General Evolution Equation for Space-Jump or Kangaroo Processes

We generalize the simple random walk as follows. Suppose that the waiting times between successive jumps are independent and identically distributed. Let $\mathscr{T}$ be the waiting time between jumps and let $\phi(t)$ be the probability density function (PDF) for the waiting time distribution (WTD). If a jump has occurred at $t = 0$ then

$$\phi(t) = \Pr\{t < \mathscr{T} \leq t + dt\}.$$

The cumulative distribution function for the waiting times is $\Phi(t) = \int_0^t \phi(s)\, ds = \Pr\{\mathscr{T} \leq t\}$ and the complementary cumulative distribution function is $\hat{\Phi}(t) = \Pr\{\mathscr{T} \geq t\} = 1 - \Phi(t)$. If the jumps are exponentially distributed then $\Phi(t) = 1 - e^{-\lambda t}$, and $\phi(t) = \lambda e^{-\lambda t}$, and this is the only smooth distribution for which the jump process is Markovian ([31], p. 458).

In general the jumps in space may depend on the waiting time, and conversely, the WTD may depend on the size of the preceding jump, but to make the analysis tractable, we assume that the spatial redistribution that occurs at jumps is independent of the WTD. Let $T(\mathbf{x}, \mathbf{y})$ be the PDF for a jump from $\mathbf{y}$ to $\mathbf{x}$, i.e., given that a jump occurs at T_i,

$$T(\mathbf{x}, \mathbf{y})\, d\mathbf{x} = \Pr\{\mathbf{x} \leq X(T_i^+) \leq \mathbf{x} + d\mathbf{x} \;\; | X(T_i^-) = \mathbf{y}\}, \tag{28}$$

where the superscripts $\pm$ denote limits from the right and left, respectively. If the underlying medium is spatially non-homogeneous and anisotropic, the transition probability depends on $\mathbf{x}$ and $\mathbf{y}$ separately, while in a homogeneous medium $T(\mathbf{x}, \mathbf{y}) = \tilde{T}(\mathbf{x} - \mathbf{y})$, where $\tilde{T}$ is the unconditional probability of a jump of length $|\mathbf{x} - \mathbf{y}|$. In either case, T is a probability kernel if and only if $\int_{R^n} T(\mathbf{x}, \mathbf{y})\, d\mathbf{x} = 1$. We further assume that T is a smooth function and that for any fixed $\mathbf{y}$ the first two

x- moments of T are finite, though they depend on **y** unless the system is spatially homogeneous. Later we comment on the effect of infinite moments.

Let $P(\mathbf{x}, t|0)d\mathbf{x}$ be the probability that a jumper which begins at the origin at $t = 0$ is in the interval $(\mathbf{x}, \mathbf{x} + d\mathbf{x})$ at time t. It was shown in [73] that $P(\mathbf{x}, t|0)$ satisfies the renewal equation

$$P(\mathbf{x}, t|0) = \hat{\Phi}(t)\delta(\mathbf{x}) + \int_0^t \int_{R^n} \phi(t-\tau)T(\mathbf{x}, \mathbf{y})P(\mathbf{y}, \tau|0)\, d\mathbf{y}\, d\tau. \tag{29}$$

Many of the standard jump processes can be recovered from this general result by particular choices of ϕ and T. For instance, if $\phi(t) = \delta(t - t_0)$ then $\Phi(t) = H(t_0 - t)$, where $H(\cdot)$ is the Heaviside function, and (29) reduces to

$$P(\mathbf{x}, t|0) = H(t_0 - t)\delta(\mathbf{x}) + [1 - H(t_0 - t)] \int_{R^n} T(\mathbf{x}, \mathbf{y})P(\mathbf{y}, t - t_0|0)\, d\mathbf{y}.$$

This is the governing equation for a discrete time, continuous space process in which jumps occur at intervals of t_0. If in addition the support of T is concentrated on the points of a lattice $Z^n \subset R^n$, then

$$P(\mathbf{x}_i, t|0) = H(t_0 - t)\delta_{i0} + [1 - H(t_0 - t)] \sum_j T_{ij} P(\mathbf{x}_j, t - t_0|0)\,.$$

where δ_{i0} is the Kronecker delta, and $\mathbf{x}_i$ is a lattice point. This can be written in the more conventional Chapman-Kolmogorov form as follows.

$$P_{i0}(n+1) = \textstyle\sum_j T_{ij} P_{j0}(n) \qquad n \geq 1$$

If the WTD is exponential, one obtains the continuous time random walk

$$\frac{\partial P}{\partial t}(\mathbf{x}, t|0) = -\lambda P(\mathbf{x}, t|0) + \lambda \int_{R^n} T(\mathbf{x}, \mathbf{y})P(\mathbf{y}, t|0)\, d\mathbf{y}. \tag{30}$$

and if in addition the support of the kernel $T(\mathbf{x}, \mathbf{y})$ is a lattice then

$$\frac{\partial P}{\partial t}(\mathbf{x}_i, t|0) = -\lambda P(\mathbf{x}_i, t|0) + \lambda \sum_j T_{ij} P(\mathbf{x}_j, t|0). \tag{31}$$

One can cast the latter into the form of a master equation for a countable state Markov process by applying the condition on T that guarantees conservation of walkers to obtain

$$\frac{\partial P}{\partial t}(\mathbf{x}_i, t|0) = -\lambda \sum_i T_{ij} P(\mathbf{x}_i, t|0) + \lambda \sum_j T_{ij} P(\mathbf{x}_j, t|0). \tag{32}$$

A generalization of this that allows for other non-exponential WTDs takes the form

$$\frac{\partial P}{\partial t}(\mathbf{x}_i, t|0) = \int_0^t \Psi(t-\tau)\left[-\sum_i T_{ij}\, P(\mathbf{x}_i, t|0) + \sum_j T_{ij}\, P(\mathbf{x}_j, t|0)\right] d\tau, \quad (33)$$

and of course one can couple the jump probabilities with the WTD [53].

There is a large literature on the various special cases. For instance, the continuous-time random walk (CTRW) dates at least back to Irwin [48] and has been extensively developed for birth-death processes [40] and on lattices [54,66,98]. The general form (29) was first derived in [73].

3.3 The Evolution of Spatial Moments for General Kernels

To determine how the evolution of the spatial moments in time depends on the waiting time distribution, we assume that the medium is one-dimensional and spatially homogeneous—the generalization to n dimension is straightforward. Let

$$\begin{aligned}\langle x^n(t)\rangle &= \int_{-\infty}^{+\infty} x^n\, P(x,t|0)\, dx \\ &= \int_{-\infty}^{+\infty}\int_0^t \int_{-\infty}^{+\infty} x^n \tilde{T}(x-y)\phi(t-\tau)\, P(y,\tau|0)\, dy\, d\tau\, dx. \end{aligned} \quad (34)$$

Denote by

$$m_k = \int_{-\infty}^{+\infty} x^k \tilde{T}(x)\, dx$$

the k-th moment about zero of the jump length distribution—then as shown in [73]

$$\langle x^n(t)\rangle = \int_0^t \sum_{k=0}^{n} \binom{n}{k} m_k \phi(t-\tau)\langle x^{n-k}(\tau)\rangle\, d\tau, \quad (35)$$

and thus the Laplace transform of the k-th moment is given by

$$X_n = \frac{\bar{\phi}(s)}{1-\bar{\phi}(s)}\left[\sum_{k=1}^{n-1}\binom{n}{k} m_k X_{n-k} + \frac{m_n}{s}\right].$$

In particular the first two moments are

$$\begin{aligned} X_1(s) &= \frac{m_1}{s}\frac{\bar{\phi}(s)}{1-\bar{\phi}(s)} \\ X_2(s) &= \left(2m_1 X_1(s) + \frac{m_2}{s}\right)\frac{\bar{\phi}(s)}{1-\bar{\phi}(s)}. \end{aligned} \quad (36)$$

The two most widely-used waiting time distributions are the exponential distribution and the gamma distribution. Suppose in either case that $m_1 = 0$, since a non-zero first moment simply adds a drift. Then for the exponential WTD one finds that $\bar{\phi}(s) = \lambda/(s+\lambda)$ and that $\langle x^2(t)\rangle = m_2\lambda t$. If ϕ is a gamma WTD with parameters $(2,\lambda)$, then $\phi(t) = \lambda^2 t e^{-\lambda t}$, $\bar{\phi}(s) = \lambda^2/(s+\lambda)^2$, and

$$\langle x^2(t)\rangle = m_2 \int_0^t \mathscr{L}^{-1}\left(\frac{\lambda^2}{s(s+2\lambda)}\right) d\tau = \frac{m_2\lambda}{2}\left\{t - \frac{1}{2\lambda}(1-e^{-2\lambda t})\right\}. \quad (37)$$

In general the asymptotic behavior of the moments can be gotten by applying limit theorems for Laplace transforms [99]. If we denote the kth moment of the WTD as M_k and suppose that $m_1 = 0$, then the leading terms in an asymptotic expansion of $X_2(s)$ are

$$X_2 = \frac{m_2}{M_1 s^2}\left[1 + \left(\frac{M_2 - 2M_1^2}{2M_1}\right)s + \mathscr{O}(s^2)\right].$$

Therefore, by (i) applying the limit result that $\lim_{s\to 0} f(s) = \lim_{t\to\infty} F(t)$, and (ii) using the fact that

$$\mathscr{L}(t^{\rho-1}) = \frac{\Gamma(\rho)}{s^\rho} \qquad \text{for} \quad \rho > 0,$$

one sees that if the mean waiting time M_1 is finite, then the mean-squared displacement for large t is given by

$$\langle x^2(t)\rangle \sim \frac{m_2}{M_1}t.$$

Thus so far as the mean-squared displacement is concerned, any jump process for which the jump distribution has a finite variance and the WTD has a finite mean behaves like a diffusion process with diffusion coefficient $D = m_2/(2M_1)$ for large t.

To make the connection with the PDE descriptions of motion more explicit, consider first the case of an exponential WTD, and suppose that the jump kernel is spatially homogeneous. If

$$\tilde{T}(\mathbf{x}-\mathbf{y}) = \frac{\delta(|\mathbf{x}-\mathbf{y}|-\ell)}{\omega_n \ell^{n-1}},$$

where $\omega_n = 2\pi^{\frac{n}{2}}/\Gamma(\frac{n}{2})$ is the surface measure of the unit sphere in R^n, one finds that

$$\frac{\partial P}{\partial t} = \lambda[\bar{P}(\mathbf{x},\ell,t) - P(\mathbf{x},t)],$$

where $\bar{P}$ is the average of P over the surface of a sphere of radius ℓ centered at $\mathbf{x}$. Expansion of P about $\mathbf{x}$ leads, in the diffusion limit $\lambda \to \infty, \ell \to 0, \lambda\ell^2/2n = D$, to

$$\frac{\partial P}{\partial t} = D\nabla^2 P, \tag{38}$$

provided that all higher-order derivatives are bounded. The Pearson walk described earlier falls into this class.

A similar conclusion holds for more general kernels, written in 1D for simplicity, of the form

$$\tilde{T}(x-y) = \frac{1}{\ell} T_0\left(\frac{|x-y|}{\ell}, \ell\right).$$

Then

$$\frac{\partial P}{\partial t} = \lambda\left(\ell \int_R T_0(r,\ell) r dr\right)\frac{\partial P}{\partial x} + \lambda\left(\frac{\ell^2}{2}\int_R T_0(r,\ell) r^2 dr\right)\frac{\partial^2 P}{\partial x^2} + \mathcal{O}(\ell^3). \tag{39}$$

Therefore if the first moment of T_0 is $\mathcal{O}(\ell)$ for $\ell \to 0$, if the second moment of T_0 tends to a constant, and if all higher moments are bounded, then in the diffusion limit we obtain a diffusion equation with drift. The diffusion coefficient is given by

$$D = \lambda\frac{\ell^2}{2}\lim_{\ell\to 0}\int_R T_0(r,\ell) r^2 dr \tag{40}$$

and the drift coefficient is given by

$$\beta = \lambda\frac{\ell^2}{2}\lim_{\ell\to 0}\int_R \frac{T_0(r,\ell)}{\ell} r dr. \tag{41}$$

The latter vanishes if the kernel is symmetric.

3.4 The Effects of Long Waits or Large Jumps

The fact that any jump process with a WTD that has a finite first moment and a jump distribution having a finite second moment evolves like a standard Brownian motion for large t is simply a reflection of the central limit theorem applied to the sum of the IID steps taken in the walk [51]. When the large-time limit of the mean-square displacement grows either sub- or super-linearly the process is said to exhibit anomalous diffusion. For example, if

$$\langle x^2(t)\rangle \sim \gamma t^\beta$$

for $\beta \neq 1$ and $t \to \infty$, it is called *subdiffusion* if $\beta < 1$ and *superdiffusion* if $\beta > 1$ [65]. Subdiffusion occurs when particles spread slowly, whether because they rest or are trapped for a long time, and in particular, if the mean waiting time between jumps is infinite. For example, if $m_1 = 0$, then from (36)

$$\langle x^2(t)\rangle = m_2 \mathscr{L}^{-1}\left(\frac{\bar{\phi}(s)}{s(1-\bar{\phi}(s))}\right).$$

Therefore, if $\bar{\phi}(s) \sim 1/s^\rho$ for $\rho \in (0,1)$ and $s \to 0$, then $\langle x^2(t)\rangle \sim m_2 t^\rho$ for $t \to \infty$, i.e., movement is asymptotically subdiffusive. As another example, consider

$$\phi(t) = \frac{1}{(1+t)^2},$$

which is a well-defined distribution, but for which $M_k = \infty$ for all $k \geq 1$. The transform of ϕ is

$$\bar{\phi}(s) = \left(\frac{\pi}{2} - Si(s)\right)\cos s + Ci(s)\sin s$$

where Si and Ci are the sine and cosine integral functions [20]. From the asymptotic expansion of the integrals one finds that

$$\langle x^2(t)\rangle \sim \log t,$$

and thus the process is subdiffusive.

The superdiffusive case arises when the walk is highly persistent in time, for example, if the walker never changes direction, or for walks having a fat-tailed jump distribution. The simplest example of the first case arises when the walker never turns, which leads to a wave equation for which the mean square displacement scales as t^2. More generally this arises if $\bar{\phi}(s) \sim \Gamma(3)/(s^2 + \Gamma(3))$ for $s \to 0$. An application to bacteria that exhibit long runs is discussed in [64].

The latter case arises when the variance of the jump distribution diverges and the central limit theorem does not apply. The motion corresponds to a Lévy flight, which leads to alternate localized meandering punctuated by occasional long steps. A comparison of a Lévy flight for the jump distribution

$$\tilde{T}(\mathbf{x}) = A_\mu \frac{\sigma}{(\sigma|\mathbf{x}|)^{1+\mu}}$$

for $\mu = 1.5$ with Brownian motion is shown in Fig. 3. The applicability of Lévy flights as a description of animal movement is discussed in [26].

Fig. 3 An example of Brownian motion (*lower left*) in the X–Y plane, and a Lévy walk (*upper right*) (From [65])

3.5 Biased Jumps Dependent on Gradients or Internal Dynamics

Several generalizations of the preceding examples are possible. The WTD for the jump process can depend on time or on the density of individuals, the redistribution kernel may depend on the local density or a local average of the density, and of course the WTD and jump distributions need not be independent. Examples of the latter case include introduction of a resting phase in which the resting time depends on the preceding jump length, or alternatively, the WTD distribution may depend directly on the jump length. It is known that a resting phase with Poisson driven entry and exits simply rescales the diffusion coefficient in simple random walks [46, 98].

If the waiting time distribution depends on the number density n and t, then

$$\phi(n,t) = \lambda(n(\mathbf{x},t),t)e^{-\int_0^t \lambda(n(\mathbf{x},s),s)\,ds}.$$

and the renewal equation for the number density is now the nonlinear equation

$$n(\mathbf{x},t) = e^{-\int_0^t \lambda(n(\mathbf{x},s),s)\,ds} F(\mathbf{x}) + \int_0^t \int_R \lambda(n(\mathbf{x},t-\tau),t-\tau)e^{-\int_0^{t-\tau} \lambda(n(\mathbf{x},s),s)\,ds} T(\mathbf{x},\mathbf{y})n(\mathbf{y},\tau)\,d\mathbf{y}\,d\tau.$$

For suitable choices of the dependence on the density this can describe either aggregation or dispersal. Dispersal at high densities would obtain if $\lambda(n,\cdot)$ is an increasing function of n, in which case the mean waiting time between jumps is a decreasing function n. On the other hand, density-dependent aggregation could be modeled using a λ that decreases with n, in which case the waiting time between

jumps increases with the density. A different approach in which the parameters depend on internal state variables will be discussed later.

The kernel T may also depend on external fields such as the concentration of an attractant and on the internal state of the organism, and one expects this dependence to be reflected in the resulting limit equations. This will be discussed in greater detail in the context of velocity-jump processes, but here we briefly illustrate the issue for space-jump processes.

Let $\mathbf{x} = x\boldsymbol{\xi}$ and $\mathbf{y} = y\boldsymbol{\eta}$, where $\boldsymbol{\xi}$ and $\boldsymbol{\eta}$ are the directions of $\mathbf{x}$ of $\mathbf{y}$. For a fixed $\mathbf{y}$, the average $\mathbf{x}$ after a jump is defined as

$$\overline{\mathbf{x}} = \int T(\mathbf{x}, \mathbf{y})\mathbf{x}\, d\mathbf{x} = \int T(\mathbf{x}, \mathbf{y})\xi x^n\, dx\, d\omega_n.$$

The angle between $\overline{\boldsymbol{\xi}}$ and $\boldsymbol{\eta}$ measures the tendency for the next jump to remain aligned with $\boldsymbol{\eta}$. Therefore we define an index of directional persistence as

$$\psi_d \equiv \langle \overline{\boldsymbol{\xi}}, \boldsymbol{\eta} \rangle, \tag{42}$$

and clearly $\psi_d \in [-1, +1]$. If the step lengths are fixed at Δ, as in the Pearson walk, and if the turning probability depends only on the cone angle

$$\theta(\mathbf{x}, \mathbf{y}) \equiv \cos^{-1}(\langle \boldsymbol{\xi}, \boldsymbol{\eta} \rangle)$$

between $\mathbf{y}$ and $\mathbf{x}$, then $T(\mathbf{x}, \mathbf{y})$ has the form

$$T(\mathbf{x}, \mathbf{y}) = \frac{\delta(|\mathbf{x} - \mathbf{y}| - \Delta)}{\Delta^{n-1}} h(\theta(\mathbf{x}, \mathbf{y}))$$

for any $n \geq 2$ and a normalized distribution h.

To illustrate how external fields can be incorporated we write

$$T(\mathbf{x}, \mathbf{y}) = \tilde{T}_0(x - y) + T_1(\mathbf{x}, \mathbf{y}),$$

and we suppose that the drift in $\tilde{T}_0$ vanishes, that the bias kernel T_1 has compact support and vanishing first moment, and that

$$\int_{R^n} T_1(\mathbf{x}, \mathbf{y}) P(\mathbf{y}) d\mathbf{y} = \int_{B_\delta(\mathbf{x})} (\mathbf{y} - \mathbf{x}) \cdot \mathbf{F}(S(\mathbf{y})) P(\mathbf{y}) d\mathbf{y}.$$

Here S is a specified field, $\mathbf{F}$ is a vector-valued function of S, and $B_\delta(\mathbf{x})$ is a ball of radius δ, the sensing radius, centered at $\mathbf{x}$. For example, let $\mathbf{F} = -\chi \nabla S$, define $\mathbf{y} - \mathbf{x} = \boldsymbol{\rho}$, and expand around $\mathbf{x}$; then one finds that

$$\int_{R^n} T_1(\mathbf{x},\mathbf{y})P(\mathbf{y})d\mathbf{y} = -\gamma\left[\nabla S(\mathbf{x})\nabla P(\mathbf{x}) + P(\mathbf{x})\nabla\nabla S(\mathbf{x})\right] : \int_{B_\delta(\mathbf{x})} \boldsymbol{\rho}\boldsymbol{\rho} d\boldsymbol{\rho} \quad (43)$$

$$= -\gamma V_n \delta^3 \left[\nabla S(\mathbf{x})\nabla P(\mathbf{x}) + P(\mathbf{x})\nabla\nabla S(\mathbf{x})\right] : \boldsymbol{\delta} \quad (44)$$

where

$$V_n = \pi^{\frac{n}{2}}/\Gamma(\frac{n}{2}+1)$$

is the volume of B_1 in n dimensions, and $\boldsymbol{\delta}$ is the unit second rank isotropic tensor [71]. Thus the n-dimensional extension of the drift-free version of (39) to include the bias given above reads

$$\frac{\partial P}{\partial t} = D\Delta P - \chi\left(\nabla S \cdot \nabla P + P\nabla\cdot\nabla S\right), \quad (45)$$

which is a form of the chemotaxis equation discussed later.

3.6 Aggregation in Reinforced Random Walks

The rigorous analysis of random walks is more complicated when particle interactions, either direct or indirect, are taken into account (cf. [68, 88, 89]). As will be discussed later, *E. coli* releases a diffusible attractant, whereas myxobacteria gliding on a slime trail react to their own contribution to these trails and to the contributions of the other bacteria [101]. There is a growing mathematical literature on what are called reinforced random walks that began with the work of Davis [24]; a recent review can be found in [82]. Here we sketch the approach developed in [72], where the particle motion is governed by a jump process and the walkers modify the transition probabilities on intervals for subsequent transitions of an interval.

Davis [24] considered a reinforced random walk for a single particle in one dimension. Initially there is a weight w_n^i on each interval $(i, i+1)$, $i \in \mathbb{Z}$ which is equal to w_n^0.[1] If at time n an interval has been crossed by the particle exactly k times, its weight will be

$$w_n^i = w_n^0 + \sum_{j=1}^{k} a_j,$$

where $a_j \geq 0$, $j = 1, \ldots, k$. Furthermore, the transition probabilities are given by

$$P(x_{i+1} = n+1 | x_i = n) = \frac{w_n^i}{w_n^i + w_{n-1}^i}.$$

[1] In this section the weight w may be equivalent to the signal S used earlier, or some function of it.

Davis' main theorem asserts that localization of the particle will occur if the weight on the intervals grows rapidly enough with each crossing, as summarized in the following. Let x_i be the particle position at the ith step, let $X \equiv \{x_i, i \geq 0\}$, and let

$$\text{and} \quad \phi(a) \equiv \sum_{n=1}^{\infty} \left(1 + \sum_{i=1}^{n} a_i\right)^{-1}.$$

Theorem 1. *Suppose that* $w_n^0 = 1$. *Then*

(i) If $\phi(a) = \infty$ *then* X *is recurrent.*
(ii) If $\phi(a) < \infty$ *then* X *has finite range and there are random integers* n *and* I *such that* $x_i \in (n, n+1)$ *if* $i > I$.

Here recurrent means that every integer is visited infinitely often a.s., i.e., the walker does not become trapped. From this it follows that if $a_j = $ constant, for instance, which corresponds to linear growth of the weight, then X is recurrent almost surely, whereas if the growth is superlinear then the particle oscillates between two random integers almost surely after some random elapsed time. Since the result deals with a single particle it does not directly address the aggregation problem, but it does suggest that if the particles interact only through the modification of the transition probability there may be aggregation if this modification is strong enough.

This theorem motivated the following development, in which we begin with a master equation for a continuous-time, discrete-space random walk. and postulate a generalized form of (31) in which the transition rates depend on the density of a control or modulator species that modulates the transition rates [72]. We restrict attention to one-step jumps, although it is easy, using the framework given earlier, to apply this to general graphs, but one may not obtain diffusion equations in the continuum limit.

Suppose that the conditional probability $p_n(t)$ that a walker is at $n \in \mathbb{Z}$ at time t, conditioned on the fact that it begins at $n = 0$ at $t = 0$, evolves according to the continuous time master equation

$$\frac{\partial p_n}{\partial t} = \hat{\mathcal{T}}_{n-1}^{+}(W)\, p_{n-1} + \hat{\mathcal{T}}_{n+1}^{-}(W)\, p_{n+1} - (\hat{\mathcal{T}}_n^{+}(W) + \hat{\mathcal{T}}_n^{-}(W))\, p_n. \tag{46}$$

Here $\hat{\mathcal{T}}_n^{\pm}(\cdot)$ are the transition probabilities per unit time for a one-step jump to $n \pm 1$, and $(\hat{\mathcal{T}}_n^{+}(W) + \hat{\mathcal{T}}_n^{-}(W))^{-1}$ is the mean waiting time at the nth site. We assume throughout that these are nonnegative and suitably smooth functions of their arguments. The vector W is given by

$$W = (\cdots, w_{-n-1/2}, w_{-n}, w_{-n+1/2}, \cdots, w_o, w_{1/2}, \cdots). \tag{47}$$

Note that the density of the control species w is defined on the embedded lattice of half the step size. The evolution of w will be considered later; for now we assume that the distribution of w is given. Clearly a time- and p-independent spatial

distribution of w can model a heterogeneous environment, but this static situation is not treated here.

As (46) is written, the transition probabilities can depend on the entire state and on the entire distribution of the control species. Since there is no explicit dependence on the previous state the jump process may appear to be Markovian, but if the evolution of w_n depends on p_n, then there is an implicit history dependence, and the space jump process by itself is not Markovian. However, if one enlarges the state space by appending w one obtains a Markov process in this new state space.

Three distinct types of models are developed and analyzed in [72], which differ in the dependence of the transition rates on w; (i) strictly local models, (ii) barrier models, and (iii) gradient models. In the first of these the transition rates are based on local information, so that $\hat{\mathscr{T}}_n^{\pm} = \hat{\mathscr{T}}(w_n)$, and to simplify the analysis we assume that the jumps are symmetric, i.e., that $\hat{\mathscr{T}}^+ = \hat{\mathscr{T}}^- \equiv \hat{\mathscr{T}}$. In this case (46) reduces to

$$\frac{\partial p_n}{\partial t} = \hat{\mathscr{T}}(p_{n-1}, w_{n-1})p_{n-1} + \hat{\mathscr{T}}(p_{n+1}, w_{n+1})p_{n+1} - 2\hat{\mathscr{T}}(p_n, w_n)p_n.$$

If we assume that there is a scaling of the transition rates such that $\hat{\mathscr{T}} = \lambda\mathscr{T}$, and that the formal diffusion limit

$$\lim_{\substack{h\to 0\\ \lambda\to\infty}} \lambda h^2 = \text{ constant} \equiv D$$

exists, we obtain the nonlinear diffusion equation

$$\frac{\partial p}{\partial t} = D\frac{\partial^2}{\partial x^2}(\mathscr{T}(w)p). \tag{48}$$

The second type is one called a barrier model, for which there are two sub-cases, depending on whether or not the transition rates are re-normalized. In the first case one assumes that $\hat{\mathscr{T}}_n^{\pm}(W) = \hat{\mathscr{T}}(w_{n\pm 1/2})$, which leads to the equation

$$\frac{\partial p}{\partial t} = D\nabla\cdot(\mathscr{T}\nabla p).$$

If one re-normalizes the transition rates so that

$$\lambda(\hat{\mathscr{T}}_n^{+}(W) + \hat{\mathscr{T}}_n^{-}(W)) = constant \equiv \lambda,$$

then after some analysis one finds that in the diffusion limit this leads to

$$\frac{\partial p}{\partial t} = D\frac{\partial}{\partial x}\left(p\frac{\partial}{\partial x}\left(\ln\frac{p}{\mathscr{T}}\right)\right). \tag{49}$$

Table 1 Dependence of the response on the sensing mechanism

	Type of sensing	Taxis velocity	Chemotactic sensitivity	Type of taxis
1.	Local	$-D\nabla\mathscr{T}$	$-D\mathscr{T}'(w)$	Negative if $\mathscr{T}'(w) > 0$
2.	Barrier without re-normalization	0	0	None
3.	Barrier with re-normalization	$D\nabla ln\mathscr{T}$	$D\,(\ln\mathscr{T}(w))'$	Positive if $\mathscr{T}'(w) > 0$
4.	Nearest neighbor with re-normalization	$2D\nabla ln\mathscr{T}$	$2D\,(\ln\mathscr{T}(w))'$	Positive if $\mathscr{T}'(w) > 0$
5.	Gradient without re-normalization	$2D\beta\nabla\tau$	$2D\beta\tau'(w)$	Positive if $\beta\tau'(w) > 0$
6.	Gradient with re-normalization	$D\frac{\beta}{\alpha}\nabla\tau$	$D\frac{\beta}{\alpha}\tau'(w)$	Positive if $\beta\tau'(w) > 0$

For later comparison with velocity jump processes we define the chemotactic velocity and sensitivity as

$$\chi = D\,(\ln\mathscr{T})_w \qquad u = -D\frac{\partial}{\partial x}\ln p + D\,(\ln\mathscr{T}(w))'\frac{\partial w}{\partial x}. \tag{50}$$

Thus the taxis is positive if $\mathscr{T}'(w) > 0$. The simplest form of w-dependence is to assume that $\mathscr{T}(w) = \alpha + \beta w$, and we use this form later in examples.

The last type of sensing leads to the gradient-based, or look-ahead model, for which $T^+_{n-1} = \alpha + \beta(\tau(w_n) - \tau(w_{n-1}))$ and $T^-_{n+1} = \alpha + \beta(\tau(w_n) - \tau(w_{n+1}))$, $\alpha \geq 0$, and again there are two cases, depending on whether or not the rates are re-normalized. The chemotactic velocities and sensitivities for these and the preceding cases are summarized in Table 1.

Of course we also have to specify the local dynamics for the evolution of w, and here we use the general form

$$\frac{\partial w}{\partial t} = \frac{pw}{1+\lambda w} + \gamma_r\frac{p}{K+p} - \mu w \equiv R(p,w) \tag{51}$$

in the examples shown in Fig. 4. For all cases we set $D = 0.36$, and in the first panel we show the solution of (49) and (51) for $\alpha = \gamma_r = \mu = 0$ and $\beta = 1, \lambda = 10^{-5}$. The second panel is as in the first, but with $\lambda = 0$, and in the third panel a more complicated transition rate is used (cf. [72]). One sees in that figure that both the dependence of the transition rates on the local modulator w, and the dynamics of w itself, play an important role in the dynamics of the system. In the first panel the solution stabilizes at some smooth distribution, in the second panel the solution blows up in finite time (around t = 9.3—this assertion is supported by analysis of

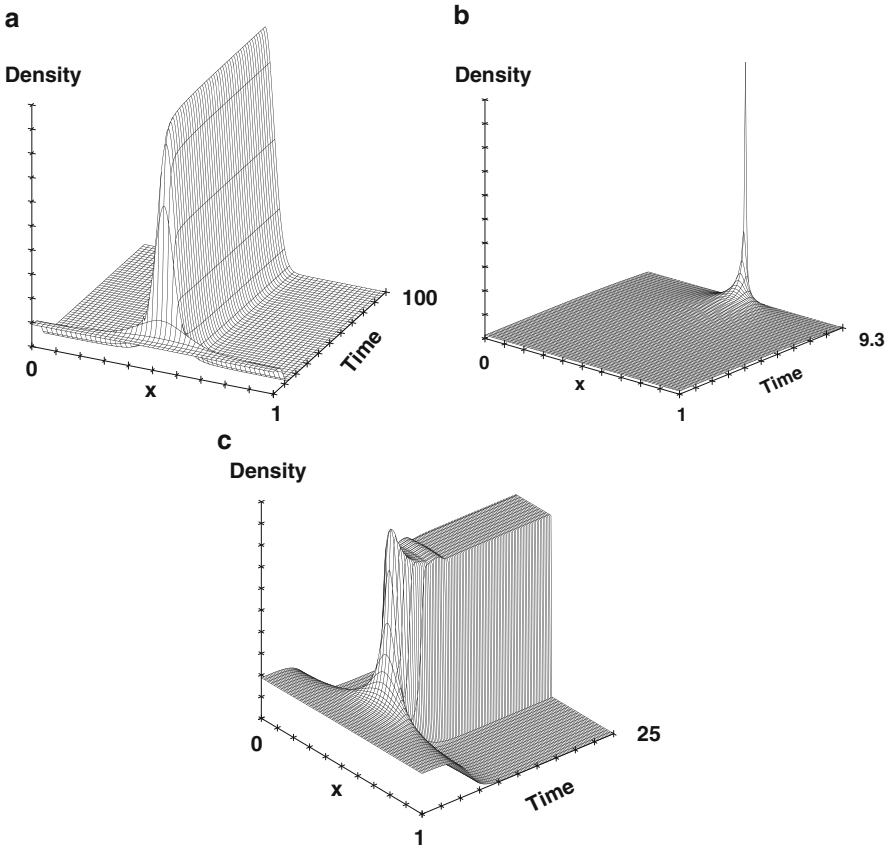

Fig. 4 The density profiles from three examples of the local dynamics. Reproduced from [72], copyright 1997 Society for Industrial and Applied Mathematics

the Fourier components—see [72]) and in the third panel the solution ultimately collapses, in a very interesting step-wise fashion that is not understood at present.

The analysis of reinforced random walks presented in [72] can be generalized in many directions. For example, consider the re-normalized transition rates

$$\hat{\mathscr{T}}_n^{\pm}(w) = \frac{w_{n\pm 1/2}}{w_{n+1/2} + w_{n-1/2}}. \tag{52}$$

These can be regarded as the discrete version of the continuous forms

$$\hat{\mathscr{T}}^{+}(w) = \frac{\frac{1}{h}\int_x^{x+h} w(s)ds}{\frac{1}{h}\left[\int_{x-h}^{x+h} w(s)ds\right]}$$

$$\hat{\mathscr{T}}^{-}(w) = \frac{\frac{1}{h}\int_{x-h}^{x} w(s)ds}{\frac{1}{h}\int_{x-h}^{x+h} w(s)ds}.$$

The continuous version implies that the walker averages over the interval $(x, x+h)$ or $(x-h, x)$ to determine the transition rate. Of course one can incorporate a more general kernel. For example, one might use

$$\hat{\mathscr{T}}^{\pm}(w(x)) = \pm \frac{\int_x^{\infty} \lambda^2 (y-x)^2 e^{-\lambda^2 (y-x)^2} \; w(y)\, dy}{\int_{-\infty}^{\infty} \lambda^2 (y-x)^2 e^{-\lambda^2 (y-x)^2} \; w(y)\, dy}$$

which assigns the maximum weight to $x \pm 1/\lambda$. More generally, we may simply assume that

$$\hat{\mathscr{T}}^{+}(w(x)) = \frac{\int_x^{\infty} K(y-x,h)\, w(y)\, dy}{\int_x^{\infty} K(y-x,h)\, w(y)\, dy + \int_{-\infty}^{x} K(x-y,h) w(y)\, dy}$$

$$\hat{\mathscr{T}}^{-}(w(x)) = \frac{\int_{-\infty}^{x} K(x-y,h)\, w(y)\, dy}{\int_x^{\infty} K(y-x,h) w(y)\, dy + \int_{-\infty}^{x} K(x-y,h) w(y)\, dy}$$

for a suitable kernel K. To recover (52) we choose

$$K(y-x,h) = \delta(y-x-\frac{h}{2}).$$

4 Velocity Jump Processes and Taxis Equations

As described in Sect. 2, the velocity-jump (VJ) process is predicated on the assumption that particles make instantaneous jumps in velocity space, rather than in physical space [73]. By comparing the underlying basis of the FPKK equation with that of the Smoluchowski equation, one should expect that the VJ process gives rise to evolution equations that depend jointly on physical- and velocity-space operators. Just as the FPKK equation leads to the Smoluchowski equation in certain regimes, it is known that the long-time asymptotics of VJ processes lead to diffusion processes in space under suitable scalings of space and time [1,41,77]. In this section we define the general VJ process and summarize results on diffusion limits of this process. In the last subsections we describe the application of this process to two classes of biological organisms—swimming bacteria and crawling cells.

4.1 The General Velocity-Jump Process

We shall work directly with the differential equation form of the conservation equation for a phase space density function that depends only on the position, velocity, time and some intracellular variables. In essence the resulting equation is the analog of the Liouville equation (19) with an additional term to account for

the gain or loss of particles at a point in phase space due to the underlying jump process. Throughout we focus on the evolution of a smooth density function, and do not address the question of how to connect this to limiting forms of the empirical density for an N-particle system.

Let $p(\mathbf{x}, \mathbf{v}, \mathbf{y}, t)$ be the density function for individuals in a $2n + m$-dimensional phase space with coordinates $(\mathbf{x}, \mathbf{v}, \mathbf{y})$, where $\mathbf{x} \in \mathbb{R}^n$ is the position of an individual, $\mathbf{v} \in \mathbb{R}^n$ is its velocity, and $\mathbf{y}$ is the set of intracellular state variables involved in cell movement. The evolution of p is governed by the equation

$$\frac{\partial p}{\partial t} + \nabla_{\mathbf{x}} \cdot (\mathbf{v} p) + \nabla_{\mathbf{v}} \cdot (\mathbf{F} p) + \nabla_{\mathbf{y}} \cdot (\mathbf{f} p) = \mathscr{R}, \tag{53}$$

where $\mathbf{F}$ denotes an external, velocity-independent force acting on the individuals, $\mathbf{f}$ is the rate of change of the internal variable $\mathbf{y}$, and $\mathscr{R}$ is the rate of change of p due to birth/death processes, a jump process that generates random changes of velocity, etc. Normally cell proliferation is independent of the velocity, and the rate of proliferation can be approximated by $r(n)p$, where $r(n)$ is the density-dependent growth rate, but here we only include random velocity changes. In addition we assume that cells are sufficiently separated and neglect cell-cell mechanical interactions.

The jump process for velocity changes is the direct analog of the stochastic process underlying space jumps. Initially we suppose that the waiting time between jumps and the changes in velocity are independent, and that the WTD is exponential. As a result, the turning can be described by two quantities, the turning rate λ, and the turning kernel $T(\mathbf{v}, \mathbf{v}')$, which defines the probability of a change in velocity from $\mathbf{v}'$ to $\mathbf{v}$, given that a reorientation occurs. $T(\mathbf{v}, \mathbf{v}')$ is non-negative and normalized so that $\int T(\mathbf{v}, \mathbf{v}')\, d\mathbf{v} = 1$, and at present we assume that it is independent of time and space. In light of the foregoing assumptions, (53) becomes

$$\frac{\partial p}{\partial t} + \nabla_{\mathbf{x}} \cdot (\mathbf{v} p) + \nabla_{\mathbf{v}} \cdot (\mathbf{F} p) + \nabla_{\mathbf{y}} \cdot (\mathbf{f} p) = -\lambda p + \lambda \int T(\mathbf{v}, \mathbf{v}') p(\mathbf{x}, \mathbf{v}', t)\, d\mathbf{v}', \tag{54}$$

and the underlying stochastic process is called a *velocity jump process*. For most purposes one does not need the distribution p, but only its first few velocity moments. The first three are the observable density of individuals $n(\mathbf{x}, t)$, the momentum, and the momentum flux.

$$n(\mathbf{x}, t) = \int p(\mathbf{x}, \mathbf{v}, \mathbf{y}, t) \mathrm{d}\mathbf{v}\mathrm{d}\mathbf{y}, \quad \mathbf{j}(\mathbf{x}, t) = \int p(\mathbf{x}, \mathbf{v}, \mathbf{y}, t) \mathbf{v}\, \mathrm{d}\mathbf{v}\mathrm{d}\mathbf{y}$$

$$\mathbf{P} = \int p(\mathbf{x}, \mathbf{v}, \mathbf{y}, t) \mathbf{v}\mathbf{v}\, \mathrm{d}\mathbf{v}\mathrm{d}\mathbf{y}.$$

The momentum $\mathbf{j}$ defines the average velocity $\mathbf{u} = \mathbf{j}/n$. Integration of (54) over $(\mathbf{v}, \mathbf{y})$ leads to

$$\frac{\partial n}{\partial t} + \nabla_{\mathbf{x}} \cdot n\mathbf{u} = 0. \tag{55}$$

When λ is independent of $\mathbf{y}$, multiplication of (54) by $\mathbf{v}$ and integration over $(\mathbf{v}, \mathbf{y})$ yields

$$\frac{\partial(n\mathbf{u})}{\partial t} + \nabla \cdot \mathbf{P} - \mathbf{F}n = -\lambda n\mathbf{u} + \lambda \int T(\mathbf{v}, \mathbf{v}')\mathbf{v}p(\mathbf{x}, \mathbf{v}', \mathbf{y}, t)\, d\mathbf{v}' d\mathbf{v} d\mathbf{y}. \tag{56}$$

These are not closed, except in a special case noted later, due to the presence of the momentum flux tensor $\mathbf{P}$ and the integral term on the right. Until stated otherwise, we assume that $\mathbf{F} = \mathbf{0}$.

It is observed experimentally that the movement of cells often exhibits directional persistence, and as a result, the turning kernel depends on the angle θ between the previous velocity $\mathbf{v}'$ and the new direction $\mathbf{v}$ [8, 39, 59, 62]. Let s denote the cell speed, and $\mathbf{e_v}$ denote the direction of the velocity, then, $\mathbf{v} = s\mathbf{e_v}$. For a fixed $\mathbf{v}'$, the average velocity $\mathbf{v}$ after reorientation is defined as

$$\bar{\mathbf{v}} = \int T(\mathbf{v}, \mathbf{v}')\mathbf{v}\, d\mathbf{v} = \int T(\mathbf{v}, \mathbf{v}')s^n \mathbf{e_v}\, ds\, d\omega_n$$

and the average speed is

$$\bar{s} \equiv \int T(\mathbf{v}, \mathbf{v}') \parallel \mathbf{v} \parallel \, d\mathbf{v} = \int T(\mathbf{v}, \mathbf{v}')s^n\, ds\, d\omega_n.$$

As in the space-jump framework, we characterize persistence via an index of directional persistence, defined as

$$\psi_d \equiv \frac{\bar{\mathbf{v}} \cdot \mathbf{v}'}{\bar{s}s'} \in [-1, +1], \tag{57}$$

which measures the tendency of the motion to persist in a given direction $\mathbf{e_{v'}}$. Of particular interest is the case in which the speed does not change with reorientation and the turning probability depends only on θ. Then $T(\mathbf{v}, \mathbf{v}')$ has the form

$$T(\mathbf{v}, \mathbf{v}') = h\left(\theta(\mathbf{v}, \mathbf{v}')\right) \tag{58}$$

for any $n \geq 2$. For such T, ψ_d is independent of $\mathbf{v}'$ and

$$\bar{\mathbf{v}} = \psi_d \mathbf{v}', \tag{59}$$

where

$$\psi_d = \begin{cases} 2\int_0^\pi h(\theta)\cos\theta\, d\theta & \text{for } n = 2 \\ 2\pi\int_0^\pi h(\theta)\cos\theta\sin\theta\, d\theta & \text{for } n = 3. \end{cases} \tag{60}$$

Observations of the movement of *Dictyostelium discoideum* (Dd) amoeba yield $\psi_d \approx 0.7$ [39], whereas the three-dimensional bacterial random walk data in [8] show $\psi_d \approx 0.33$.

External signals enter either through a direct effect on the turning rate λ and the turning kernel T, or indirectly via internal variables $\mathbf{y}$ that reflect the external signal and in turn influence λ and/or T. The first case arises when experimental results are used to directly estimate parameters in the equation [32], but the latter approach is more fundamental. The reduction of (54) to the macroscopic chemotaxis equations for the first case is done in [41, 70], and second case is done in [28–30, 104, 105]. In [104], external forces are also included. We summarize some of the important aspects of the reduction in the following sections.

4.2 The Telegraph Process

A simple example will illustrate both the reduction of the jump process to a diffusion process, and how the parameters of the jump process have to be controlled so as to produce aggregation. Suppose that the walkers are confined to the real line $\mathbb{R}$, that the speeds $s^{\pm}$ to the right and left may depend on position, and that direction is reversed at random instants governed by Poisson processes of intensity $\lambda^{\pm}$. Let $p^{\pm}$ denote the density of walkers moving to the right and left, respectively. Then the conservation equations for these densities are[2]

$$\begin{aligned} \frac{\partial p^+}{\partial t} + \frac{\partial (s^+ p^+)}{\partial x} &= -\lambda^+ p^+ + \lambda^- p^-, \\ \frac{\partial p^-}{\partial t} - \frac{\partial (s^- p^-)}{\partial x} &= \lambda^+ p^+ - \lambda^- p^-. \end{aligned} \tag{61}$$

Let $n \equiv p^+ + p^-$ be the macroscopic density and note that the flux j is $(s^+ p^+ - s^- p^-)$; then (61) can be written in the alternative form

$$\begin{aligned} &\frac{\partial n}{\partial t} + \frac{\partial j}{\partial x} = 0, \\ &\frac{\partial j}{\partial t} + s^+ \frac{\partial (s^+ p^+)}{\partial x} + s^- \frac{\partial (s^- p^-)}{\partial x} = (s^+ + s^-)(-\lambda^+ p^+ + \lambda^- p^-). \end{aligned} \tag{62}$$

To illustrate the essence of aggregation and taxis in this simple context, we ask how the walkers should modify their behavior so as to produce a nonuniform distribution in space at steady-state, and we consider three cases.

[2]These equations are the restriction of (54) to one-space dimension only when the speeds $s^{\pm}$ are constant, and in that case the moment equations close at the second level for constant λ [73]. We consider the more general case for illustrative purposes.

Case I: Constant and equal turning rates and speeds, $\lambda^+ = \lambda^- = \lambda_0$ and $s^+(x) = s^-(x) = s_0$

By combining the two equations at (62) we obtain the classical telegrapher's equation

$$\frac{\partial^2 n}{\partial t^2} + 2\lambda_0 \frac{\partial n}{\partial t} = s^2 \frac{\partial^2 n}{\partial x^2}, \tag{63}$$

and by formally taking the limit $\lambda_0 \to \infty, s \to \infty$ with $s^2/\lambda_0 \equiv 2D$ constant in (63), one obtains the diffusion equation. However the limiting procedure can be made more precise by considering the exact solution of (63), which is

$$n(x,t) = \begin{cases} \dfrac{e^{-\lambda_0 t}}{2}\left(\delta(x-st) + \delta(x+st) + \dfrac{\lambda_0}{s}\left[I_0(\Lambda) + \dfrac{\lambda_0 t}{\Lambda} I_1(\Lambda)\right]\right) + n_0 & |x| \le st, \\ n_0 & |x| > st. \end{cases}$$

Here I_0 and I_1 are modified Bessel functions of the first kind. By applying the asymptotic expansions

$$I_0(z) = \frac{e^z}{\sqrt{2\pi z}} + \mathcal{O}\left(\frac{1}{z}\right), \qquad I_1(z) = \frac{e^z}{\sqrt{2\pi z}} + \mathcal{O}\left(\frac{1}{z}\right), \qquad \text{as } z \to \infty,$$

one finds that

$$n(x,t) = \frac{1}{\sqrt{4\pi D t}} e^{-\dfrac{x^2}{4Dt}} + n_0 + e^{-\lambda_0 t}\mathcal{O}(\xi^2), \qquad \xi^2 \equiv (x/st)^2.$$

From this one sees that the telegraph process reduces to a diffusion process on space scales that are small compared with the ballistic scale st. This fact was known to Einstein and this process has since been studied by many [34, 37, 49, 73, 92].

If we define $\tau = \epsilon^2 t$ and $\xi = \epsilon x$, where ϵ is a small parameter, then (63) reduces to

$$\epsilon^2 \frac{\partial^2 n}{\partial \tau^2} + 2\lambda_0 \frac{\partial n}{\partial \tau} = s^2 \frac{\partial^2 n}{\partial \xi^2}. \tag{64}$$

In these coordinates $x/(st) = \epsilon\xi/(s\tau)$ and the diffusion regime only requires that $\xi/(s\tau) \le \mathcal{O}(1)$. In the limit $\epsilon \to 0$ the exact solution can be used to show that (64) again reduces to the diffusion equation, both formally and rigorously (for t bounded away from zero). However this shows that the approximation of the telegraph process by a diffusion process hinges on the appropriate relation between the space and time scales, not necessarily on the limit of speed and turning rate tending to infinity. In any case, it is clear that the spatial distribution of n is asymptotically constant, and thus there is no localization of walkers. Imposing no-flux boundary conditions on a finite interval does not change this conclusion.

Case II: Constant and equal turning rate $\lambda^+ = \lambda^- = \lambda_0$, distinct speed $s^+(x) \neq s^-(x)$

By assuming that the flux j at infinity vanishes, and solving for the steady state solutions of (61), one finds that

$$p^+(x) = \left[\frac{s^+(0)p^+(0)}{s^+(x)}\right] e^{\lambda_0 \int_0^x \frac{s^+ - s^-}{s^+ s^-} d\xi},$$

$$p^-(x) = \left[\frac{s^+(0)p^+(0)}{s^-(x)}\right] e^{\lambda_0 \int_0^x \frac{s^+ - s^-}{s^+ s^-} d\xi},$$

where the constant $p^+(0)$ is the cell density moving to the right at $x = 0$, which is determined from the conservation of total particle number. From this we see that, (a) aggregation can occur when the speed of the cell depends on the spatial location, i.e., $s^\pm$ are not constants, (b) the distributions for the right-moving cells and the left-moving cells differ if $s^+(x) \neq s^-(x)$, and (c) if $s^+ = s^-$, both left- and right-moving cells aggregate at points of low speed. This is somewhat similar to the scenario of traffic flow—when the road becomes narrower, cars slow down, and traffic jams may form.

Case III: Distinct turning rates $\lambda^+(x) \neq \lambda^-(x)$, constant and equal speeds $s^+ = s^- = s_0$

We write

$$\lambda^\pm = \frac{\lambda^+ + \lambda^-}{2} \pm \frac{\lambda^+ - \lambda^-}{2} =: \lambda_0 \pm \lambda_1,$$

then the density-flux form (62) becomes

$$\begin{aligned} \frac{\partial n}{\partial t} + \frac{\partial j}{\partial x} &= 0, \\ \frac{\partial j}{\partial t} + s^2 \frac{\partial n}{\partial x} &= -2\lambda_0 j - 2s\lambda_1 n. \end{aligned} \tag{65}$$

When λ_0 is constant this reduces to

$$\frac{\partial^2 n}{\partial t^2} + 2\lambda_0 \frac{\partial n}{\partial t} = s^2 \frac{\partial^2 n}{\partial x^2} - 2s \frac{\partial}{\partial x}(\lambda_1 n). \tag{66}$$

We call this a hyperbolic aggregation or taxis equation, and we will see later how this emerges in general. The difference of the turning rate produces a drift in the dynamical evolution equal to $u_c = s\lambda_1/\lambda_0$. This is similar to what is observed in a 1D space-jump process when the probability of right and left jumps differ.

The steady-state solution of (65) is

$$n(x) = n_0 \exp\left\{-\frac{2}{s}\int_0^x \lambda_1(\xi)d\xi\right\},$$

and again there may be a non-constant solution, which is a result of the difference in turning of cells.

We see from the simple 1D process that non-uniform cell distributions can arise when either the cell speeds are different or the turning rates are different, and these two cases correspond to what are called chemotaxis and chemokinesis, resp. In particular, in case 4.2 cells aggregate where their speed is lowest, which is the case when amoeboid cells reach the peak of a potential attractant, while in case 4.2 cells aggregate most strongly when the turning rate deviation λ_1 returns to zero, which happens when run-and-tumble cells adapt to the signal gradient.

4.3 Reduction of the VJ Process to a Diffusion Process

In general, in higher space dimensions equations (55) and (56) do not specify n and $\mathbf{u}$ as they stand, for they involve the second $\mathbf{v}$ moment of p and the as yet unspecified kernel $T(\mathbf{v}, \mathbf{v}')$. We call the process unbiased when the turning rate and kernel depend only on $\mathbf{v}$ and $\mathbf{v}'$, and biased when external fields or internal state variables are included. Note that an unbiased kernel does not mean that reorientation is isotropic. We assume hereafter that λ is independent of the velocity, and we write (54) for the unbiased process as

$$\frac{\partial}{\partial t}p(\mathbf{x},\mathbf{v},t) + \mathbf{v}\cdot\nabla p(\mathbf{x},\mathbf{v},t) = -\lambda p(\mathbf{x},\mathbf{v},t) + \lambda\int_V T_0(\mathbf{v},\mathbf{v}')p(\mathbf{x},\mathbf{v}',t)d\mathbf{v}' \equiv \mathscr{L}_0 p(\mathbf{x},\mathbf{v},t). \tag{67}$$

We consider the spatial domain $\Omega = \mathbb{R}^n$, and we suppose that the velocities lie in a compact set $V \subset \mathbb{R}^n$ that is symmetric with respect to the origin.

To state some of the results from [41], we let $\mathscr{K}$ denote the cone of nonnegative functions in $L^2(V)$, and for fixed $(\mathbf{x}, t)$ define an integral operator $\mathscr{T}$ and its adjoint $\mathscr{T}^*$ by

$$\mathscr{T}\, p = \int_V T(\mathbf{v},\mathbf{v}')p(\mathbf{x},\mathbf{v}',t)d\mathbf{v}', \qquad \mathscr{T}^*\, p = \int_V T(\mathbf{v}',\mathbf{v})p(\mathbf{x},\mathbf{v}',t)d\mathbf{v}'. \tag{68}$$

We impose the following conditions on the kernel and the integral operator:

(T1) $T(\mathbf{v},\mathbf{v}') \geq 0$, $\int_V T(\mathbf{v},\mathbf{v}')d\mathbf{v} = 1$, and $\int_V\int_V T^2(\mathbf{v},\mathbf{v}')d\mathbf{v}'d\mathbf{v} < \infty$.

(T2) *There are functions* u_0, ϕ, *and* $\psi \in \mathscr{K}$ *with* $u_0 \not\equiv 0$ *and* $\phi, \psi \neq 0$ *a.e. such that for all* $(\mathbf{v},\mathbf{v}') \in V \times V$

$$u_0(\mathbf{v})\phi(\mathbf{v}') \leq T(\mathbf{v}',\mathbf{v}) \leq u_0(\mathbf{v})\psi(\mathbf{v}'). \tag{69}$$

(T3) $\|\mathscr{T}\|_{\langle 1\rangle^\perp} < 1$, where $\langle 1\rangle^\perp$ is the orthogonal complement in $L^2(V)$ of the span of 1.
(T4) $\int_V T(\mathbf{v},\mathbf{v}')d\mathbf{v}' = 1$.

Then the turning operator $\mathscr{L}_0 p(\mathbf{x},\mathbf{v},t)$ acts in $L^2(V)$, and has the following spectral properties [41].

Theorem 2. *Assume* (T1)–(T4)*; then the following hold.*

1. 0 *is a simple eigenvalue of* $\mathscr{L}_0$*, and the corresponding eigenfunction is* $\phi(\mathbf{v}) \equiv 1$.
2. *There is a decomposition* $L^2(V) = \langle 1\rangle \oplus \langle 1\rangle^\perp$*, and, for all* $\psi \in \langle 1\rangle^\perp$*,*

$$\int_V \psi \mathscr{L}_0 \psi d\mathbf{v} \le -\mu_2 \|\psi\|^2_{L^2(V)}, \quad \textit{where} \quad \mu_2 \equiv \lambda(1 - \|\mathscr{T}\|_{\langle 1\rangle^\perp}). \tag{70}$$

3. *All nonzero eigenvalues* μ *satisfy* $-2\lambda < \mathrm{Re}\ \mu \le -\mu_2 < 0$*, and to within scalar multiples there is no other positive eigenfunction.*
4. $\|\mathscr{L}_0\|_{\mathbf{L}(L^2(V),L^2(V))} \le 2\lambda$.
5. $\mathscr{L}_0$ *restricted to* $\langle 1\rangle^\perp \subset L^2(V)$ *has an inverse* $\mathscr{F}$ *with norm*

$$\|\mathscr{F}\|_{\mathbf{L}(\langle 1\rangle^\perp,\langle 1\rangle^\perp)} \le \frac{1}{\mu_2}. \tag{71}$$

If for example the turning kernel $T(\mathbf{v},\mathbf{v}')$ is symmetric, then the constant μ_2 given in (70) is the negative of the second eigenvalue of the turning operator $\mathscr{L}_0$. This defines a time scale for relaxation of the reorientation process, and in particular, if 1 is not a simple eigenvalue of $\mathscr{T}$, the streaming character of the transport process dominates, and we can no longer expect to obtain a diffusion limit.

Under the preceding assumptions the parabolic scaling $\tau = \epsilon^2 t$ and $\xi = \epsilon\mathbf{x}$, where ϵ is a small dimensionless parameter, leads to a diffusion approximation of the transport equation [41]. In these variables we have

$$\epsilon^2 \frac{\partial p}{\partial \tau} + \epsilon \mathbf{v}\cdot\nabla_\xi\, p = -\lambda p + \lambda \int_V T(\mathbf{v},\mathbf{v}')p(\boldsymbol{\xi},\mathbf{v}',\tau)d\mathbf{v}'. \tag{72}$$

where the subscript on ∇, which we drop hereafter, indicates differentiation with respect to the scaled space variable. The right-hand side of (72) is $\mathscr{O}(1)$ compared with the left-hand side, whatever the magnitude of p, and this leads to a diffusion equation for the lowest order term p_0 of an outer expansion, which we write as

$$p(\boldsymbol{\xi},\mathbf{v},\tau) = \sum_{i=0}^{k} p_i(\boldsymbol{\xi},\mathbf{v},\tau)\epsilon^i + \epsilon^{k+1} p_{k+1}(\boldsymbol{\xi},\mathbf{v},\tau). \tag{73}$$

An approximation result for any order in ϵ that provides a bound on the difference between the solution of the transport equation and an expansion derived from the solution of the associated parabolic diffusion equation has also been proven.

Theorem 3. *[41] Assume* (T1)–(T4) *and the Hilbert expansion (73), where* p_0 *solves the parabolic limit equation*

$$\frac{\partial p_0}{\partial \tau} - \nabla \cdot \left(D \nabla p_0 \right) = 0, \qquad p_0(\boldsymbol{\xi}, 0) = \int_V p(\boldsymbol{\xi}, \mathbf{v}, 0) d\mathbf{v}, \tag{74}$$

with diffusion tensor

$$D = -\frac{1}{\omega} \int_V \mathbf{v} \mathscr{F} \mathbf{v} d\mathbf{v}. \tag{75}$$

In addition, the higher order corrections are given by

$$p_1 = \mathscr{F}(\mathbf{v} \cdot \nabla p_0), \qquad p_2 = \mathscr{F}(p_{0,\tau} + \mathbf{v} \cdot \nabla \mathscr{F} \mathbf{v} \cdot \nabla p_0),$$

where $\mathscr{F}$ *is the pseudoinverse defined in Theorem 2 and* $\omega = |V|$*. Then, for each* $\vartheta > 0$*, there exists a constant* $C > 0$ *such that for each* $\vartheta/\epsilon^2 < t < \infty$ *and each* $x \in \mathbb{R}^n$

$$\| p(x, ., t) - q_2(\epsilon x, ., \epsilon^2 t) \|_{L^2(V)} \leq C \, \epsilon^3,$$ [3]

and the constant C *depends on* μ_2, V, D*, and* ϑ*.*

In general, the approximate solution depends only on the solution of the limiting parabolic equation, and, therefore, it cannot be uniformly valid in time (cf. [41]). When the speed is constant and the outgoing directions are uniformly distributed on S^{n-1}, $\mathscr{F} = -\lambda^{-1}$, and

$$D = \frac{1}{\omega} \int_V \frac{\mathbf{v}\mathbf{v}}{\lambda} d\mathbf{v} = \frac{s^2}{\lambda n} I.$$

One can prove in general that the diffusion tensor is positive definite, and one can also derive necessary and sufficient conditions for it to be a scalar multiple of I.

Since the reduction depends critically on the existence of the parabolic scaling, we give an example of how it is determined. Let L be a characteristic scale associated with the macroscopic evolution, for instance, the size of the domain on which an experiment is done. Define the dimensionless velocity, space and time variables

$$\mathbf{u} = \frac{\mathbf{v}}{s} \quad \boldsymbol{\xi} = \frac{\mathbf{x}}{L} \quad \tau = \frac{t}{\sigma},$$

where s is a characteristic speed and σ is as yet undetermined. Then

$$\frac{1}{\sigma} \frac{\partial p}{\partial \tau} + \left(\frac{s}{L} \right) \mathbf{u} \cdot \nabla^* p = -\lambda p + \lambda \int T(\mathbf{u}, \mathbf{u}') p(\boldsymbol{\xi}, \mathbf{u}', \tau) d\mathbf{u}',$$

[3] In [41] this estimate appears with the L^2-norm squared, but it is clear from the proof that there should be no square.

We estimate a diffusion coefficient as the product of the characteristic speed times the average distance traveled between velocity jumps, which gives $D \sim \mathcal{O}(s^2/\lambda)$, and a characteristic drift time

$$\tau_{DIFF} \sim \frac{L^2}{D} = \frac{L^2\lambda}{s^2}, \qquad \tau_{DRIFT} = \frac{L}{s},$$

A characteristic speed for bacteria such as *E. coli* is 10–20 μ/s, and $\lambda^{-1} \sim \mathcal{O}(1)$ s. On a length scale of 1 mm $\tau_{DRIFT} \sim$ 50–100 s and $\tau_{DIFF} \sim 2,500 - 10^4$ s. Therefore, in this example we have $\tau_{RUN} \sim \mathcal{O}(1)$ on the dimensional scale, and

$$\tau_{DRIFT} \sim O(1/\epsilon), \qquad \tau_{DIFF} \sim O(1/\epsilon^2)$$

where $\epsilon \sim \mathcal{O}(10^{-2})$. Then

$$\tau_{RUN} \equiv \lambda^{-1} \ll \tau_{DRIFT} \ll \tau_{DIFF}$$

and the scaled equation results for $\sigma = \tau_{DIFF}$.

When biases are introduced their magnitude relative to the base turning rate is critical. We write the kernel with bias as $T(\mathbf{v}, \mathbf{v}', p(\cdot))$, and if, for example, we assume the bias is linear in a signal gradient, then

$$T(\mathbf{v}, \mathbf{v}', p(\cdot)) = T_0(\mathbf{v}, \mathbf{v}') + \kappa(\mathbf{v} \cdot \nabla p)(\mathbf{v}' \cdot \nabla p).$$

One finds that

$$D(\boldsymbol{\xi}, \tau) = \frac{s^2}{\lambda_0 n}\left(I + \frac{\omega s^2}{n}\kappa \nabla p \, \nabla p \left(I - \frac{\omega s^2}{n}\kappa \nabla p \, \nabla p\right)^{-1}\right),$$

and as expected, there is no drift or taxis in this case.

On the other hand, if the perturbation is $\mathcal{O}(\epsilon)$, and linear in the gradient, then one finds that

$$\frac{\partial p_0}{\partial \tau} = \nabla \cdot (D \nabla p_0 - u_c p_0),$$

where the drift or chemotactic velocity is given by

$$\mathbf{u}_c \equiv -\frac{\lambda_0}{\omega}\int\int v \mathcal{F}_0 T_1(\mathbf{v}, \mathbf{v}') d\mathbf{v}' d\mathbf{v}.$$

Here F_0 denotes the pseudo inverse defined by the kernel T_0. If Q_1 has the particular form

$$Q_1 = k_1(\mathbf{v}', S)\mathbf{v}$$

then

$$\chi(p) = k(p)\frac{s^2}{\omega n}.$$

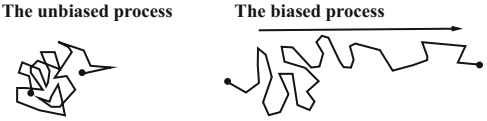

Fig. 5 The movement of a particle driven by a VJ process, in the absence (*left*) and presence (*right*) of an external bias

and the lowest-order approximation is the solution of

$$\frac{\partial p_0}{\partial \tau} = \nabla \cdot \left(\frac{s^2}{n} \nabla p_0 - p_0 \chi(p) \nabla p \right).$$

4.4 The Role of Internal Dynamics

The most widely-studied examples of organisms whose motion can be described as a velocity jump process are the flagellated bacteria, the most-studied of which is *E. coli*. *E. coli* generates the force needed for swimming by rotating flagella embedded in the cell membrane, and thus the swimming speed is fixed by the hydrodynamic loading, and can be taken to be essentially constant in a specified medium. To search for food or escape an unfavorable environment, *E. coli* alternates two basic behavioral modes, swimming in a more or less straight line called a run, and a highly erratic motion called tumbling, the purpose of which is to reorient the cell. Run times are typically much longer than the time spent tumbling, and when bacteria move in a favorable direction (i.e., either in the direction of foodstuffs or away from harmful substances) the run times are increased further. Conversely, when bacteria move in an unfavorable direction the run length decreases and the relative frequency of tumbling increases. The distribution of new directions is not uniform on the unit sphere, but has a bias in the direction of the preceding run. The effect of alternating these two modes of behavior, and in particular, of increasing the run length when moving in a favorable direction, is that a bacterium executes a three-dimensional random walk with drift in a favorable direction when observed on a sufficiently long time scale [9, 56] (cf. Fig. 5).

To illustrate the main points involved in the inclusion of internal dynamics in macroscopic equations, we begin with a simple example based on *E. coli*, and assume that there is no interaction between cells. This is a reasonable assumption, since typical bacterial densities are of the order of 10^8/ml and individual bacteria have a volume per cell of order $\pi \mu m^3$—thus the volume fraction is $\mathcal{O}(10^{-3})$. Therefore we can consider either the probability of a single walker being at a given position with a given velocity at time t, or the density of walkers, and we choose the latter here.

New technology has led to extensive experimental data at the cell and molecular level, and as a result, more complete descriptions of inter- and intracellular signal transduction are possible for use in population-level models of *E. coli*. Detailed models of the full signal transduction network exist [87,102], but simplified cartoon models that capture the essential dynamics involved in aggregation and patterning have been used in recent studies [28, 29, 104]. By neglecting body forces and cell growth, the transport equation for the cell density becomes

$$\frac{\partial p}{\partial t} + \nabla_x \cdot (\mathbf{v}p) + \nabla_y \cdot (\mathbf{f}p) = -\lambda(\mathbf{y})p + \int_V \lambda(\mathbf{y})T(\mathbf{v}, \mathbf{v}', \mathbf{y})p(\mathbf{x}, \mathbf{v}', \mathbf{y}, t)\,\mathrm{d}\mathbf{v}', \quad (76)$$

where $\mathbf{y} = (y_1, y_2)^T$. The vector $\mathbf{y}$s encodes the excitation and adaptation response of cells to external signals, and $\lambda(\mathbf{y})$ describes the motor response. The vector $\mathbf{y}$ evolves according to

$$\frac{\mathrm{d}y_1}{dt} = \frac{G(S(\mathbf{x}, t)) - (y_1 + y_2)}{t_e}, \quad (77)$$

$$\frac{\mathrm{d}y_2}{dt} = \frac{G(S(\mathbf{x}, t)) - y_2}{t_a}, \quad (78)$$

where $G(S)$ models signal detection via surface receptors and t_e and t_a specify the excitation and adaptation time scales, with $t_e << t_a$. A complete quantitative understanding of how different parameters at the cell level influence the population dynamics involves the incorporation the entire signal transduction of bacteria, but the cartoon description can predict biological aggregations and traveling bands of bacteria (cf. Fig. 6). Other intracellular variables, such as the metabolic state, can also be included in the transport equation, and this allows for a description of nutrient dependent cell growth. The existence of traveling wave solutions in the transport equations when coupled with the signal evolution equations was established in [106]. Further analysis on the comparison of the traveling waves obtained from the classical Keller-Segel equations are presented in the chapter by Frantz and Erban.

Macroscopic equations can be derived from the above multiscale models using perturbation methods and moment closure techniques, and this has been carried out successfully for the cartoon description above. The macroscopic equation

$$\frac{\partial n}{\partial t} = \nabla \cdot \left[\frac{s^2}{N\lambda_0} \nabla n - G'(S(x,t)) \frac{bs^2 t_a}{N\lambda_0(1+\lambda_0 t_a)(1+\lambda_0 t_e)} n \nabla S \right], \quad (79)$$

with $b = -\frac{\partial \lambda}{\partial y_1}|_{y_1=0}$ and N as the space dimension was derived in 1D first in [29], and extended to 3D in [28]. The major assumption used there and in earlier papers is that the signal gradient is shallow: $G'(S)\nabla S \cdot \mathbf{v} \sim \mathcal{O}(\epsilon)\ \mathrm{sec}^{-1}$ and $t_a\lambda_0 \sim \mathcal{O}(1)$, which results in a clear separation of the microscopic time scales from the macroscopic transport and diffusion time scales. Other assumptions include

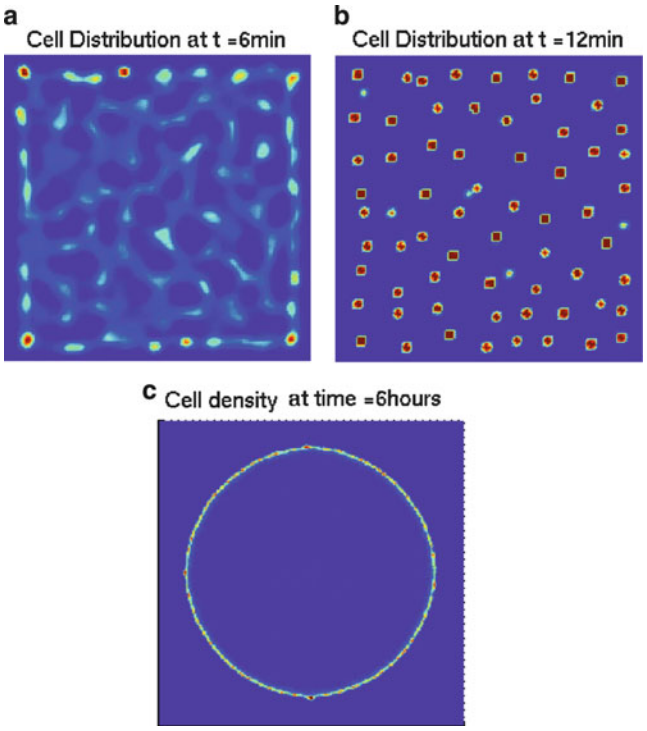

Fig. 6 Simulated *E. coli* patterns by a cell-based model. (**a**) Network formation from an uniform cell lawn; (**b**) Aggregate formation from the network; (**c**) Traveling wave formation from a single inoculum in the center. Adapted from [74] with permission

time-independent signals $S = S(\mathbf{x})$, a linear turning rate $\lambda = \lambda_0 - by_1$ and no directional persistence. From this equation one sees that if cells adapt instantly, i.e., if $t_a = 0$, then the taxis term vanishes and the population simply diffuses. In this case no aggregates will form, which is consistent with experimental observations.

New moment closure methods were developed in [104] to account for time dependent signals $S = S(\mathbf{x}, t)$ and nonlinear dependence of the turning rate on internal variables via $\lambda = \lambda_0 - by_1 + a_2 y_1^2 - \cdots$. In the general case considered there, the shallow gradient assumption becomes $\frac{b}{\lambda_0} G'(S)(\nabla S \cdot \mathbf{v} + \frac{\partial S}{\partial t}) \sim \mathcal{O}(\epsilon)\ \mathrm{s}^{-1}$. As before, the implication of this assumption is the separability of microscopic and macroscopic time scales. The same equation (79) results from the derivation, with the directional persistence appearing as a scaling of the turning rates by a factor of $1/(1-\psi_d)$. The method also applies for any finite system of internal dynamics $f(\mathbf{y})$ in polynomial form.

Chemotaxis equations in the presence of multiple signals and external forces were also derived in [104] in the context of bacterial chemotaxis. In general cells have multiple receptor types and thus can respond to many different signals. How a cell integrates these different signals and responds properly depends on the cell

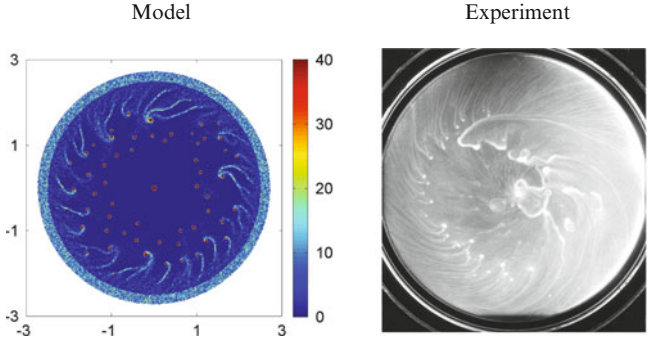

Fig. 7 Streams in a growing *Proteus mirabilis* colony. Reproduced from [107] with permission

type and is not known in general. However in bacteria different signaling pathways share the same network downstream of the receptors, and therefore different signals are integrated at the signal processing step. In this case, the function G is generally a function of all signals, $G = G(S_1, S_2, \cdots, S_m)$, and the macroscopic equation for cell density becomes

$$\frac{\partial n}{\partial t} = \nabla \cdot \left[D_n \nabla n - \chi_0 n \left(\frac{\partial G}{\partial S_1} \nabla S_1 + \cdots + \frac{\partial G}{\partial S_m} \nabla S_m \right) \right], \tag{80}$$

where

$$D_n = \frac{s^2}{N\lambda_0(1-\psi_d)},$$

and

$$\chi_0 = \frac{bs^2 t_a}{N\lambda_0(1+\lambda_0(1-\psi_d)t_a)(1+\lambda_0(1-\psi_d)t_e)}.$$

Other systems may involve separate transduction pathways for different signals, which will lead to different chemotactic sensitivities for different signals. Examples of how this affects pattern formation are given in [75].

When there are external forces that act on cells, then $\mathbf{F} \neq \mathbf{0}$ in 53, and additional terms appear in the chemotaxis equations. For example, when *E. coli* swims the flagella rotate counterclockwise when viewed from behind, and under typical conditions the Reynolds number is very small. As a result, the motion is both force and torque free, and thus the cell body must rotate clockwise. When cells swim close to a surface there is an imbalance in the viscous force between the top and bottom of the cell, which produces a clockwise swimming bias when viewed from above [25]. When this bias is incorporated into a cell-based model of aggregation, it leads to spiral density patterns as shown in Fig. 7 [107]. This was treated as a velocity-dependent force in a continuum description derived from the transport equations (54), and this led to the macroscopic chemotaxis equation

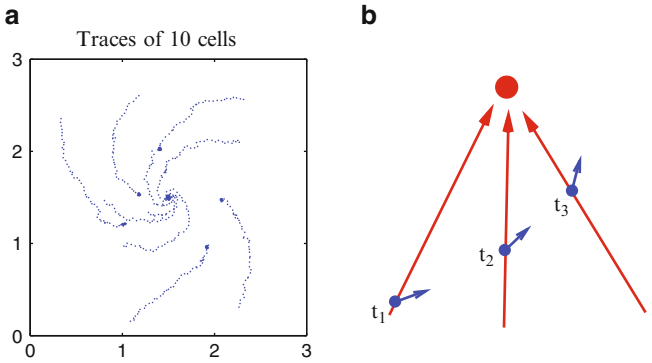

Fig. 8 (**a**) The positions of 10 randomly chosen cells from Fig. 7, each position recorded every 30 s by a *blue dot*. (**b**) the macroscopic drift given by (79) yields a qualitative explanation of the spirals. Reproduced from [107] with permission

$$\frac{\partial n}{\partial t} = \nabla \cdot \left(D_n \nabla n - G'(S) n \left(\chi_0 \nabla S + \beta_0 (\nabla S)^{\perp} \right) \right) \tag{81}$$

in two space dimensions [104]. Here $(\nabla S)^{\perp} = (\partial_{x_2} S, -\partial_{x_1} S)^T$ is a vector orthogonal to ∇S, and the diffusion coefficient and the chemotactic sensitivities, assuming fast excitation, are as follows:

$$\begin{aligned} D_n &= \frac{s^2}{2\lambda_0(1-\psi_d) + \frac{2\omega_0^2}{\lambda_0(1-\psi_d)}}, \\ \chi_0 &= \frac{b(1-\psi_d)s^2[\lambda_0(1-\psi_d)(\lambda_0(1-\psi_d)+\frac{1}{t_a}) - \omega_0^2]}{2((\lambda_0(1-\psi_d)+\frac{1}{t_a})^2 + \omega_0^2)(\lambda_0^2(1-\psi_d)^2 + \omega_0^2)}, \\ \beta_0 &= \frac{\omega_0 b(1-\psi_d)s^2(2\lambda_0(1-\psi_d)+\frac{1}{t_a})}{2((\lambda_0(1-\psi_d)+\frac{1}{t_a})^2 + \omega_0^2)(\lambda_0^2(1-\psi_d)^2 + \omega_0^2)}. \end{aligned} \tag{82}$$

The parameter ω_0 measures the swimming bias, while ψ_d is the index of directional persistence. Notice that the swimming bias decreases the diffusion coefficient and the chemotactic sensitivity χ_0, and introduces a drift or a second taxis-like term in the direction orthogonal to the signal gradient. Since the force is not velocity-independent here, the moment analysis had to be modified accordingly. The method developed in [104] can be used to incorporate the effect of more general imposed forces as well.

Equation (81) leads to an heuristic explanation of the handedness of the spirals shown in Fig. 7. This is illustrated in Fig. 8, where the traces of 10 cells are shown in (a), and the path of an individual cell is shown in (b). At $t = t_1$ the blue cell detects a signal gradient (red arrow) roughly in the 1 o'clock direction, but according to (81)

its average drift is in the direction of the blue arrow, due to the combined effects of the attractant gradient and the swimming bias. This balance is repeated at each successive time point, with the result that the cell approaches the signal source (the red dot) along an inward-spiraling, counterclockwise path as shown in (a).

As remarked earlier, (79) was derived for shallow signal gradients, i.e., $H \equiv \frac{b}{\lambda_0} G'(S)(\nabla S \cdot \mathbf{v} + \frac{\partial S}{\partial t}) \sim \mathscr{O}(\varepsilon)\ \mathrm{s}^{-1}$ with $\varepsilon = s/(L\lambda_0) \approx 10^{-2}$. It remains to be determined whether the chemotaxis equation or its variant forms gives an accurate representation of the population dynamics for bacterial chemotaxis under large spatial or temporal signal gradients. This hinges on how the macroscopic quantities relate to microscopic parameters, and, if the PKS equation fails under certain conditions, what macroscopic equation can be derived. For an ultra-small signal gradient, $H \leq \mathscr{O}(\varepsilon^2)\ \mathrm{s}^{-1}$, the chemotactic response of the population provides a small perturbation, via higher order terms, of the cell density, which evolves according to a diffusion process with $D_n = s^2/(N\lambda_0)$ [103]. For large signal gradients ($H \geq \mathscr{O}(1)\ \mathrm{s}^{-1}$) the macroscopic equation should include the nonlinear effects of the gradients in the macroscopic drift, for otherwise the linear approximation may predict a chemotactic velocity that exceeds the cell speed, which is unrealistic since there are no cell-cell or hydrodynamic interactions in the model. In this case the microscopic time scale and macroscopic time scales may overlap, and new techniques are needed to derive macroscopic equations.

In any case, the dependence of the diffusion coefficient D and the chemotactic velocity $\mathbf{u}_c$ on H can be obtained by stochastic simulations. Given different levels of H, 10^4 stochastic simulations are performed with the same initial conditions. The turning rate is given by $\lambda = \lambda_0(1 - \frac{y_1}{\gamma + |y_1|})$. The positions of the cell are recorded every half minute, and the data was analyzed to obtain the diffusion rate and the macroscopic drift. Figure 9 compares the diffusion rate and the macroscopic drift inferred from the stochastic simulations of the 2D cell-based model with the predictions from the macroscopic equation (79). It is shown that the macroscopic description gives a good approximation for $H \sim \mathscr{O}(\epsilon)\mathrm{s}^{-1}$, but the nonlinearity in the cell-based model for $H \sim \mathscr{O}(1)\mathrm{s}^{-1}$ can not be captured by the macroscopic equation with its linear dependence of H. More specificly, from the stochastic simulations, we see that the cell-based model reveals saturation in the macroscopic velocity, and gradient-dependent diffusion rates.

4.5 Macroscopic Descriptions of Eukaryotic Cell Movement

Many single-celled organisms such as *E. coli* use flagella or cilia to swim, but eukaryotic cells that lack such structures use one of two basic modes of movement—mesenchymal and amoeboid [10]. The former can be characterized as 'crawling' and involves the extension of structures whose protrusion is driven by actin polymerization at the leading edge. This mode dominates in cells such as fibroblasts when moving on a 2D substrate. In the amoeboid mode cells are more rounded and employ shape changes to move—in effect 'jostling through the crowd' or

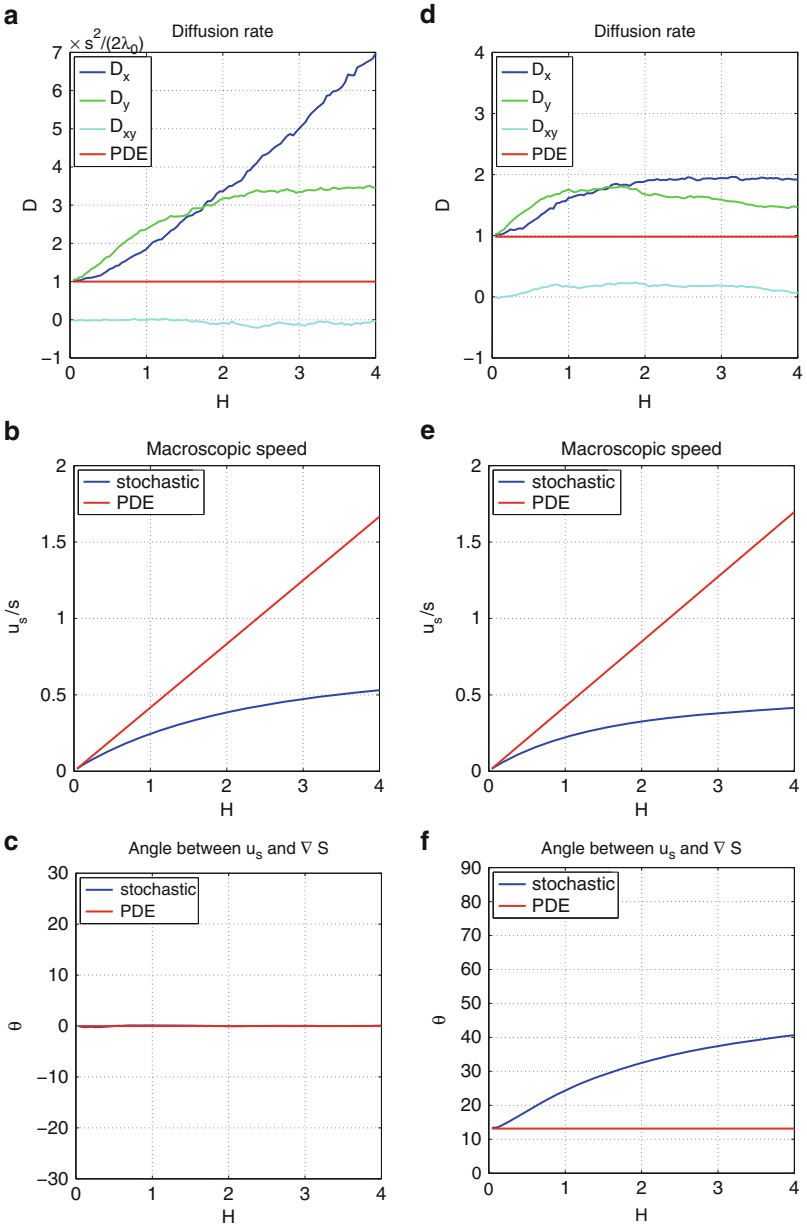

Fig. 9 A comparison of the cell-based and the macroscopic predictions of the chemotactic velocity and the diffusion coefficients in 2D. Here D_x and D_y are the diffusion coefficients perpendicular to and parallel to the signal gradient, resp., and D_{xy} is the cross diffusion coefficient. The *left column* is obtained with no swimming bias, and the *right column* is obtained with $\varepsilon_b = 0.04\pi$. Reproduced from [107] with permission

'swimming'. Leukocytes use this mode for movement through the extracellular matrix in the absence of adhesion sites [57]. Moreover, it has been shown that numerous cell types can sense the mechanical properties of their environment and adjust the balance between the modes appropriately [85]. Thus pure crawling and pure swimming are the extremes on a continuum of locomotion strategies, but many cells can choose the most effective strategy in a given context.

While 'run-and-tumble' organisms such as *E. coli* use temporal sensing to modulate their motile behavior, the motile program of eukaryotic cells such as Dd or leukocytes is more complicated. These cells are large enough to detect gradients in extracellular chemical and mechanical signals over the length of the cell, and can amplify small differences in the extracellular signal over the cell into large end-to-end intracellular differences that control the motile machinery [19, 78]. Given that these cells use spatial sensing, an individual-based model that incorporates direction sensing and movement cannot treat cells as points, but must allow for spatial variations in the finite cell volume (or area in 2D). Recent experiments show that cells in a steady gradient can polarize in the direction of the gradient without extending pseudopods [78], and thus must rely entirely on differences in the signal across the cell body for orientation. Analysis of a model for the cAMP relay pathway in Dd shows that a cell experiences a significant difference in the front-to-back ratio of cAMP when a neighboring cell begins to signal [23], which demonstrates that sufficient end-to-end differences for reliable orientation can be generated for typical extracellular signals; everything needed is that the direction-sensing pathways respond at least as fast as the cAMP pathway.

In addition to the fact that eukaryotes use spatial differences to measure signals, another major difference with 'run-and-tumble' swimmers lies in the force-generation machinery that drives the motion of eukaryotic cells. In the 'run-and-tumble' description of bacterial motion we assumed that jumps were instantaneous, which led to the velocity jump process. Furthermore, the reduction to a diffusion process can still be carried through if there is a finite lifetime in the tumble state, as long as the transitions are generated by a Poisson process [70]. In contrast, the directional changes in eukaryotic cells are much slower and depend directly on the signal location, and thus this has to be included in the model. This has been done at the single cell level, using a model for intracellular cAMP dynamics, and treating the cells as deformable viscoelastic ellipsoids that exert forces on the substrate and one another. This more complex model also produces realistic aggregation patterns [76], but there is a large gap between realistic, single-cell models and continuum descriptions. Thus far only relatively simple cell-based models have been used for the derivation of macroscopic descriptions.

One approach is to start with a Smoluchowski equation, and to postulate a relationship between the force and the chemotactic gradient. If one assumes that the motive force exerted by a cell is a function of the attractant concentration, one can compute the difference between the force at the leading and trailing edges, and then by a mean-value argument obtain a linear relation between this difference and the chemotactic gradient [79]. In this approach the chemotactic sensitivity is related to the rate of change of the force with attractant concentration. Support for this comes

from experiments which show that as many pseudopods are produced down-gradient as up, but those up-gradient are more successful in generating cell movement [93]. However, Dd and perhaps other cells, adapt to the signal, and simplified models cannot capture this effectively [43]. Thus a different approach that incorporates signal transduction and internal dynamics is needed.

In [23, 30], a cell is described as a disk ($n = 2$) or a ball ($n = 3$) $B_\varrho = \{\boldsymbol{\xi} \in \mathbf{R}^n | \ \| \boldsymbol{\xi} \| \leq \varrho\}$, and the model is formulated in terms of the position of its center $\mathbf{x} \in \mathbf{R}^n$, its velocity $\mathbf{v} \in \mathbf{R}^n$, its internal state functions $\mathbf{y} : B_\varrho \to \mathbf{R}^{d_1}$ and its membrane state functions $\mathbf{z} : \partial B_\varrho \to \mathbf{R}^{d_2}$. Denote by $\overline{\mathbf{y}} = (\mathbf{y}, \mathbf{z}) \in \mathbb{Y}$ the combined internal and membrane state, where $\mathbb{Y}$ is, in general, an infinite-dimensional Banach space.

The internal state and the acceleration are assumed to evolve according to

$$\frac{\mathrm{d}\overline{\mathbf{y}}}{\mathrm{d}t} = \mathscr{G}(\overline{\mathbf{y}}, S), \tag{83}$$

$$\frac{\mathrm{d}\mathbf{v}}{\mathrm{d}t} = \mathscr{F}(\mathbf{x}, \mathbf{v}, \overline{\mathbf{y}}), \tag{84}$$

where $\mathscr{G} : \mathbb{Y} \times \mathbb{S} \to \mathbb{Y}$ is a mapping between Banach spaces and $\mathscr{F} : \mathbf{R}^n \times \mathbf{R}^n \times \mathbb{Y} \to \mathbf{R}^n$ is the force per unit mass on the centroid. Thus the acceleration depends on the internal state. In this formulation the combined internal state $\overline{\mathbf{y}}$ includes quantities that depend on the spatial location in the cell or on the membrane, and which may, for example, satisfy a reaction-diffusion equation such as

$$\frac{\partial \mathbf{y}}{\partial t} = D\Delta\mathbf{y} + \mathbf{f}(\mathbf{y}), \text{ in } B_\varrho, \tag{85}$$

$$B(\mathbf{y}, \mathbf{z}) = 0, \qquad \text{in } \partial B_\varrho. \tag{86}$$

Thus the boundary condition for $\mathbf{y}$ depends on the membrane state functions $\mathbf{z}$, perhaps to reflect binding or other processes such as scaffold formation. The boundary variables in turn evolve according to the equation

$$\frac{\partial \mathbf{z}}{\partial t} = \mathbf{g}(\mathbf{z}, S), \qquad \text{in } \partial B_\varrho, \tag{87}$$

where S is the external signal, and this could also incorporate diffusion on the boundary by suitably altering the equation.

Given the complexity of the single cell description, it is a formidable task to derive macroscopic equations for populations of eukaryotic cells. A simple model of the form (83–84) for a single cell was analyzed in [30]. This model captures the essential features of cell movement in response to traveling waves of chemoattractant. Moreover, in that context there is a mapping $\mathscr{P} : \mathbb{Y} \to \mathbf{R}^k$, $k < \infty$, satisfying $\mathscr{F}(\mathbf{x}, \mathbf{v}, \overline{\mathbf{y}}) = \mathbf{F}(\mathbf{x}, \mathbf{v}, \mathscr{P}(\overline{\mathbf{y}}))$ where $\mathbf{F} : \mathbf{R}^n \times \mathbf{R}^n \times \mathbf{R}^k \to \mathbf{R}^n$ such that a closed evolution equation for the variable $\overline{\mathbf{z}} = \mathscr{P}(\overline{\mathbf{y}})$ can be derived. Then the cellular random walk written in terms of $(\mathbf{x}, \mathbf{v}, \overline{\mathbf{y}})$ can be equivalently formulated

in terms of the finite-dimensional state variables ($\mathbf{x}$, $\mathbf{v}$, $\overline{\mathbf{z}}$). In particular, one can formulate an equation for the probability distribution $p(\mathbf{x}, \mathbf{v}, \overline{\mathbf{z}})$ (cf. (76) written for $p(\mathbf{x}, \mathbf{v}, \mathbf{y})$ in the bacterial case). Asymptotic analysis of this transport equation leads to a system of macroscopic hyperbolic equations that accurately reflect the dynamics of the full system, but it is not known if that system can in turn be reduced to a PKS equation [30]. Other approaches have been used, e.g., generalized PKS equations have been derived beginning with a cellular Potts model [61], but the internal state plays no role in these formulations.

5 Discussion

How cells or organisms move about in space in response to signals, and how they coordinate their movement and form stationary or dynamic patterns is an important question in many biological processes, including embryonic development, cancer progression, wound healing and biofilm formation. These phenomena have been modeled in two ways in the literature. Firstly, there are continuum models based on phenomenological descriptions that lead to convection-diffusion equations such as the chemotaxis equation [42] for the evolution of the macroscopic cell density $n = n(\mathbf{x}, t)$. However, new experimental technology has advanced our knowledge on how cells detect, transduce, respond to, and propagate external stimuli, and this has led to the second approach, in which detailed cell-based models of collective cell movement towards chemical or mechanical signals [23,90,96,107] are incorporated. However, due to the complexity of intracellular dynamics and the large number of cells that are often involved, cell-based models are computationally expensive, and new techniques are needed to embed cell-level knowledge into macroscopic equations. This is a difficult problem, comparable to deriving the macroscopic rheological properties of a complex fluid such as the cytosol from knowledge of the molecular interactions, and thus not surprisingly, progress has been slow.

Here we have reviewed recent progress on deriving chemotaxis equations from space jump processes and velocity jump processes. When swimming bacteria such as *E. coli* move independently towards chemical signals, their movement can be described as independent velocity jump processes. When cells are well separated and the signal gradient is sufficiently small, chemotaxis equations are derived from the moment equations of the transport equation that describes the evolution of the cell in phase space [28–30, 41, 70, 104]. When the signal gradient is large, 1D stochastic simulations of a cell-based model show that the movement of cells is more persistent and cells run up the gradient with very little turning. Therefore statistically the diffusion rate decreases to zero, and the macroscopic velocity increases to the maximum cell speed, as the signal gradient increases. This shows that under extremely large signal gradients, the macroscopic equations for cells movement are more of a hyperbolic type, and also reflects the fact that the low-order moments in the internal dynamics cannot capture the strongly nonlinear dependence of the turning rate on the signal. This is similar to what is observed in eukaryotic cells,

which suppress random movement in the presence of strong chemotactic signals. However in 2D stochastic simulations, bacteria moving roughly orthogonal to the signal gradient still run and tumble, and this leads to diffusion coefficients that do not approach zero, in contrast with the 1D case.

There are many open problems in this area, a few of which are listed below.

- A more complete analysis of the time scales and how they depend on the external signal and the internal dynamics is needed. For example, the second eigenvalue of the turning operator controls the rate at which the diffusion regime is approached, but little has been done to obtain better estimates of the second eigenvalue based on properties of the turning kernel.
- The formulation of VJ processes herein is based on the assumption that the velocity jumps are generated by a Poisson process, but there is some evidence mentioned earlier [64] that bacteria show abnormally long run lengths that are inconsistent with this assumption. In general the non-streaming component of the transport equation (54) is simply the time derivative of the stochastic process generating the jumps, which may change depending on the signal strength, and the use of other waiting time distributions in the VJ process should be explored.
- To date most derivations of macroscopic equations from a microscopic model have ignored density effects, but these are important in examples of bacterial movement and related problems. Most analyses of density effects begin with continuum descriptions and add forces due to active motile particles [44,58], but a more fundamental approach is needed.
- In many situations, cell-cell contact and contact-induced signaling is important for collective movement. To describe this one must include cell-cell mechanical interaction terms in $\mathbf{F}$, and cell-cell contact signaling terms in the internal dynamics. A suitable starting point for this may be to add the evolution of internal dynamics to the $(\mathbf{x}, \mathbf{v})$ evolution described by the Fokker-Planck-Kramers-Klein equation (15).
- As an adjunct to this, continuum-level descriptions of tissue movement based on microscopic models, should be formulated [35], but there are many difficult homogenization issues that arise here.
- The derivation of macroscopic equations for systems when the finite-dimensional reduction $\mathscr{P} : \mathbb{Y} \to \mathbf{R}^k$ is not possible is an open problem. In fact the entire formulation as a transport equation breaks down, and a new approach is needed.

References

1. W. Alt, Biased random walk models for chemotaxis and related diffusion approximations. J. Math. Biol. **9**, 147–177 (1980)
2. D. Applebaum, *Lévy Processes and Stochastic Calculus*, vol. 93 (Cambridge University Press, Cambridge, 2004)
3. R. Aris, *Vectors, Tensors and the Basic Equations of Fluid Mechanics* (Prentice-Hall, New York, 1962)

4. L. Arnold, *Stochastic Differential Equations, Theory and applications* (Wiley-Interscience, New York, 1974)
5. L. Bachelier, *Théorie de la spéculation* (Gauthier-Villars, Paris, 1900)
6. I.L. Bajec, F.H. Heppner, Organized flight in birds. Anim. Behav. **78**(4), 777–789 (2009)
7. M.N. Barber, B.W. Ninham, *Random and Restricted Walks: Theory and Applications*, vol. 10 (Gordon and Breach, New York, 1970)
8. H.C. Berg, D.A. Brown, Chemotaxis in esterichia coli analysed by three-dimensional tracking. Nature **239**, 500–504 (1972)
9. H.C. Berg, *Random Walks in Biology* (Princeton University Press, Princeton, 1983)
10. F. Binamé, G. Pawlak, P. Roux, U. Hibner, What makes cells move: requirements and obstacles for spontaneous cell motility. Mol. BioSystems **6**(4), 648–661 (2010)
11. L. Bocquet, J. Piasecki, Microscopic derivation of non-Markovian thermalization of a Brownian particle. J. Stat. Phys. **87**(5), 1005–1035 (1997)
12. M. Born, H.S. Green, A general kinetic theory of liquids. I. the molecular distribution functions. Proc. R. Soc. Lond. Ser. A. Math. Phys. Sci. **188**(1012), 10 (1946)
13. V. Capasso, D. Bakstein, *An Introduction to Continuous-Time Stochastic Processes: Theory, Models, and Applications to Finance, Biology, and Medicine* (Birkhauser, Basel, 2005)
14. V. Capasso, D. Morale, Asymptotic behavior of a system of stochastic particles subject to nonlocal interactions. Stoch. Anal. Appl. **27**(3), 574–603 (2009)
15. J.A. Carrillo, M. Fornasier, G. Toscani, F. Vecil, Particle, kinetic, and hydrodynamic models of swarming, in *Mathematical Modeling of Collective Behavior in Socio-Economic and Life Sciences*, ed. by G. Naldi, L. Pareschi, G. Toscani. Modelling and Simulation in Science and Technology, Birkhauser (2010), pp. 297–336
16. C. Cercignani, *Mathematical Methods in Kinetic Theory*, 2nd edn. (Plenum, New York, 1969)
17. C. Cercignani, R. Illner, M. Pulvirenti, *The Mathematical Theory of Dilute Gases* (Springer, New York, 1994)
18. S. Chandrasekhar, Stochastic problems in physics and astronomy. Rev. Mod. Phys. **15**, 2–89 (1943)
19. C.Y. Chung, S. Funamoto, R.A. Firtel, Signaling pathways controlling cell polarity and chemotaxis. Trends Biochem. Sci. **26**(9), 557–566 (2001). Review
20. R.V. Churchill, *Operational Mathematics* (McGraw-Hill, New York, 1958)
21. E.A. Codling, M.J. Plank, S. Benhamou, Random walk models in biology. J. R. Soc. Interface **5**(25), 813 (2008)
22. F. Cucker, S. Smale, On the mathematical foundations of learning. Bull. Am. Math. Soc. **39**(1), 1–49 (2001)
23. J.C. Dallon, H.G. Othmer, A continuum analysis of the chemotactic signal seen by *Dictyostelium discoideum*. J. Theor. Biol. **194**(4), 461–483 (1998)
24. B. Davis, Reinforced random walks. Probab. Theory Relat. Fields **84**(2), 203–229 (1990)
25. W.R. DiLuzio, L. Turner, M. Mayer, P. Garstecki, D.B. Weibel, H.C. Berg, G.M. Whitesides, Escherichia coli swim on the right-hand side. Nature **435**(7046), 1271–1274 (2005)
26. A.M. Edwards, R.A. Phillips, N.W. Watkins, M.P. Freeman, E.J. Murphy, V. Afanasyev, S.V. Buldyrev, M.G.E. da Luz, E.P. Raposo, H.E. Stanley et al., Revisiting Lévy flight search patterns of wandering albatrosses, bumblebees and deer. Nature **449**(7165), 1044–1048 (2007)
27. A. Einstein, Über die von der molekularkinetischen Theorie der Wärme geforderte Bewegung von in ruhenden Flussigkeiten suspendierten Teilchen. Ann. der Physik **17**, 549–560 (1905)
28. R. Erban, H. Othmer, From signal transduction to spatial pattern formation in *E. coli*: a paradigm for multi-scale modeling in biology. Multiscale Model. Simul. **3**(2), 362–394 (2005)
29. R. Erban, H.G. Othmer, From individual to collective behavior in bacterial chemotaxis. SIAM J. Appl. Math. **65**(2), 361–391 (2004)
30. R. Erban, H.G. Othmer, Taxis equations for amoeboid cells. J. Math. Biol. **54**, 847–885 (2007)
31. W. Feller, *An Introduction to Probability Theory* (Wiley, New York, 1968)

32. R. Ford, D.A. Lauffenburger, A simple expression for quantifying bacterial chemotaxis using capillary assay data: application to the analysis of enhanced chemotactic responses from growth-limited cultures. Math. Biosci. **109**(2), 127–150 (1992)
33. M. Franceschetti, When a random walk of fixed length can lead uniformly anywhere inside a hypersphere. J. Stat. Phys. **127**(4), 813–823 (2007)
34. R. Fürth, Die Brownische Bewegung bei Berücksichtigung einer Persistenz der Bewegungsrichtung. Zeitsch. f. Physik **2**, 244–256 (1920)
35. J. Galle, M. Hoffmann, G. Aust, From single cells to tissue architecture-a bottom-up approach to modelling the spatio-temporal organisation of complex multi-cellular systems. J. Math. Biol. **58**(1–2), 261–283 (2009)
36. G.W. Gardiner, *Handbook of Stochastic Processes for Physics, Chemistry and Natural Sciences*, 2nd edn. (Springer, Berlin, 1985)
37. S. Goldstein, On diffusion by discontinuous movements, and on the telegraph equation. Quart. J. Mech. Appl. Math. **VI**, 129–156 (1951)
38. S.-Y. Ha, E. Tadmor, From particle to kinetic and hydrodynamic descriptions of flocking. Kinetic Relat. Model **1**(3), 415–435 (2008)
39. R.L. Hall, Amoeboid movement as a correlated walk. J. Math. Biol. **4**, 327–335 (1977)
40. C.R. Heathcote, J.E. Moyal, The random walk [in continuous time] and its application to the theory of queues. Biometrika **46**(3–4), 400 (1959)
41. T. Hillen, H.G. Othmer, The diffusion limit of transport equations derived from velocity jump processes. SIAM J. Appl. Math. **61**, 751–775 (2000)
42. T. Hillen, K.J. Painter, A users guide to PDE models for chemotaxis. J. Math. Biol. **58**(1), 183–217 (2009)
43. T. Höfer, J.A. Sherratt, P.K. Maini, Cellular pattern formation during dictyostelium aggregation. Physica D **85**(3), 425–444 (1995)
44. C. Hohenegger, M.J. Shelley, Stability of active suspensions. Phys. Rev. E **81**(4), 046311 (2010)
45. D. Horstmann, From 1970 until present: the Keller-Segel model in chemotaxis and its consequences I. Jahresbericht der DMV **105**(3), 103–165 (2003)
46. J.Hu, H.G. Othmer, A theoretical analysis of filament length fluctuations in actin and other polymers. J. Math. Biol. (2011, to appear)
47. J.M. Hutchinson, P.M. Waser, Use, misuse and extensions of "ideal gas" models of animal encounter. Biol. Rev.-Camb. **82**(3), 335 (2007)
48. J.O. Irwin, The frequency distribution of the difference between two independent variates following the same Poisson distribution. J. R. Stat. Soc. **100**(3), 415–416 (1937)
49. M. Kac, *Some Stochastic Problems in Physics and Mathematics* (Field Research Laboratory, Magnolia Petroleum Company, Dallas, 1956)
50. N. van Kampen, *Stochastic Processes in Physics and Chemistry*, 3rd edn. (North-Holland, Amsterdam, 2007)
51. S. Karlin, H. Taylor, *A First Course in Stochastic Processes* (Academic, New York, 1975)
52. E. Keller, L. Segel, Initiation of slime mold aggregation viewed as an instability. J. Theor. Biol. **26**, 399–415 (1970)
53. V.M. Kenkre, The generalized master equation and its applications, in *Statistical Mechanics and Statistical Methods in Theory and Application* (Plenum, New York, 1977)
54. V.M. Kenkre, E.W. Montroll, M.F. Shlesinger, Generalized master equations for continuous-time random walks. J. Stat. Phys. **9**(1), 45–50 (1973)
55. J.C. Kluyver, A local probability theorem. Ned. Akad. Wet. Proc. A **8**, 341–350 (1906)
56. D.E. Koshland, *Bacterial Chemotaxis as a Model Behavioral System* (Raven Press, New York, 1980)
57. T. Lämmermann, B.L. Bader, S.J. Monkley, T. Worbs, R. Wedlich-Söldner, K. Hirsch, M. Keller, R. Förster, D.R. Critchley, R. Fässler et al., Rapid leukocyte migration by integrin-independent flowing and squeezing. Nature **453**, 51–55 (2008)
58. J. Lega, T. Passot, Hydrodynamics of bacterial colonies: a model. Phys. Rev. E Stat. Nonlinear Soft Matter Phys. **67**(3 Pt 1), 031906 (2003)

59. L. Li, S.F. Nørrelykke, E.C. Cox, Persistent cell motion in the absence of external signals: a search strategy for eukaryotic cells. PLoS One **3**(5), e2093 (2008)
60. R.L. Liboff, *Kinetic Theory: Classical, Quantum, and Relativistic Descriptions* (Springer, Berlin, 2003)
61. P.M. Lushnikov, N. Chen, M. Alber, Macroscopic dynamics of biological cells interacting via chemotaxis and direct contact. Phys. Rev. E **78**(6), 061904 (2008)
62. R.M. Macnab, Sensing the environment: bacterial chemotaxis, in *Biological Regulation and Development*, ed. by R. Goldberg (Plenum Press, New York, 1980), pp. 377–412
63. U.M.B. Marconi, P. Tarazona, Nonequilibrium inertial dynamics of colloidal systems. J. Chem. Phys. **124**, 164901 (2006)
64. F. Matthaus, M. Jagodic, J. Dobnikar, E. coli superdiffusion and chemotaxis–search strategy, precision, and motility. Biophys. J. **97**(4), 946–957 (2009)
65. R. Metzler, J. Klafter, The random walk's guide to anomalous diffusion: a fractional dynamics approach. Phys. Rep. **339**(1), 1–77 (2000)
66. E.W. Montroll, G.H. Weiss, Random walks on lattices. II. J. Math. Phys. **6**, 167 (1965)
67. G. Naldi, *Mathematical Modeling of Collective Behavior in Socio-Economic and Life Sciences* (Springer, Berlin, 2010)
68. K. Oelschläger, A fluctuation theorem for moderately interacting diffusion processes. Probab. Theor. Relat. Field **74**, 591–616 (1987)
69. A. Okubo, *Diffusion and Ecological Problems: Mathematical Models* (Springer, New York, 1980)
70. H. Othmer, T. Hillen, The diffusion limit of transport equations 2: chemotaxis equations. SIAM J. Appl. Math. **62**, 1222–1250 (2002)
71. H.G. Othmer, Interactions of Reaction and Diffusion in Open Systems, PhD thesis, University of Minnesota, 1969
72. H.G. Othmer, A. Stevens, Aggregation, blowup, and collapse: The ABC's of taxis in reinforced random walks. SIAM J. Appl. Math. **57**(4), 1044–1081 (1997)
73. H.G. Othmer, S.R. Dunbar, W. Alt, Models of dispersal in biological systems. J. Math. Biol. **26**, 263–298 (1988)
74. H.G. Othmer, K. Painter, D. Umulis, C. Xue, The intersection of theory and application in biological pattern formation. Math. Mod. Nat. Phenom. **4**, 3–79 (2009)
75. K.J. Painter, P.K. Maini, H.G. Othmer, Development and applications of a model for cellular response to multiple chemotactic cues. J. Math. Biol. **41**(4), 285–314 (2000)
76. E. Palsson, H.G. Othmer, A model for individual and collective cell movement in *Dictyostelium discoideum*. Proc. Natl. Acad. Sci. **97**, 11448–11453 (2000)
77. G.C. Papanicolaou, Asymptotic analysis of transport processes. Bull. AMS **81**, 330–392 (1975)
78. C.A. Parent, P.N. Devreotes, A cell's sense of direction. Science **284**(5415), 765–770 (1999). Review
79. E. Pate, H.G. Othmer, Differentiation, cell sorting and proportion regulation in the slug stage of *Dictyostelium discoideum*. J. Theor. Biol. **118**, 301–319 (1986)
80. C.S. Patlak, Random walk with persistence and external bias. Bull. Math. Biophys. **15**, 311–338 (1953)
81. K. Pearson, The problem of the random walk. Nature **72**(1865), 294–294 (1905)
82. R. Pemantle, A survey of random processes with reinforcement. Probab. Surv. **4**, 1–79 (2007)
83. B. Perthame, Mathematical tools for kinetic equations. Bull. Am. Math. Soc. **41**(2), 205–244 (2004)
84. L. Rayleigh, On the resultant of a large number of vibrations of the same pitch and of arbitrary phase. Phil. Mag. **10**(73), 491 (1880)
85. J. Renkawitz, K. Schumann, M. Weber, T. Lämmermann, H. Pflicke, M. Piel, J. Polleux, J.P. Spatz, M. Sixt, Adaptive force transmission in amoeboid cell migration. Nat. Cell Biol. **11**(12), 1438–1443 (2009)
86. K.I. Sato, *Lévy Processes and Infinitely Divisible Distributions* (Cambridge University Press, London, 1999)

87. P.A. Spiro, J.S. Parkinson, H.G. Othmer, A model of excitation and adaptation in bacterial chemotaxis. Proc. Natl. Acad. Sci. **94**(14), 7263–7268 (1997)
88. H. Spohn, *Large Scale Dynamics of Interacting Particles* (Springer, New York, 1991)
89. A. Stevens, The derivation of chemotaxis equations as limit dynamics of moderately interacting stochastic many-particle systems. SIAM J. Appl. Math. **61**, 183–212 (2000)
90. M.A. Stolarska, Y. Kim, H.G. Othmer, Multi-scale models of cell and tissue dynamics. Phil. Trans. R. Soc. A **367**(1902), 3525 (2009)
91. D.W. Stroock, Some stochastic processes which arise from a model of the motion of a bacterium. Probab. Theor. Relat. Field **28**, 305–315 (1974)
92. G.I. Taylor, Diffusion by continuous movements. Proc. Lond. Math. Soc. **20**, 196–212 (1920)
93. B.J. Varnum-Finney, E. Voss, D.R. Soll, Frequency and orientation of pseudopod formation of *Dictyostelium discoideum* amebae chemotaxing in a spatial gradient: further evidence for a temporal mechanism. Cell Motil. Cytoskeleton **8**(1), 18–26 (1987)
94. K. Kang, B. Perthame, A. Stevens, J.J.L. Velázquez, An integro-differential equation model for alignment and orientational aggregation. J. Differ. Equat. **246**(4), 1387–1421 (2009)
95. T. Vicsek, A. Zafiris, Collective motion (2010). arXiv preprint arXiv:1010.5017
96. D.C. Walker, G.Hill, S.M. Wood, R.H. Smallwood, J. Southgate, Agent-based computational modeling of wounded epithelial cell monolayers. IEEE Trans. Nanobiosci. **3**(3), 153–163 (2004)
97. Q.D. Wang, The global solution of the n-body problem. Celestial Mech. Dynam. Astron. **50**, 73–88 (1991)
98. G.H. Weiss, *Aspects and Applications of the Random Walk*, vol. 121 (North-Holland, Amsterdam, 1994)
99. D. Widder, *The Laplace Transform* (Princeton University Press, Princeton, 1946)
100. G. Wilemski, On the derivation of Smoluchowski equations with corrections in the classical theory of Brownian motion. J. Stat. Phys. **14**(2), 153–169 (1976)
101. Y. Wu, A.D. Kaiser, Y. Jiang, M.S. Alber, Periodic reversal of direction allows myxobacteria to swarm. Proc. Natl. Acad. Sci. **106**(4), 1222 (2009)
102. X. Xin, H.G. Othmer, A trimer of dimers - based model for the chemotactic signal transduction network in bacterial chemotaxis. Bull. Math. Biol., 1–44 (2012)
103. C. Xue, Mathematical Models of Taxis-Driven Bacterial Pattern Formation, PhD thesis, University of Minnesota, 2008
104. C. Xue, H.G. Othmer, Multiscale models of taxis-driven patterning in bacterial populations. SIAM J. Appl. Math. **70**(1), 133–167 (2009)
105. C. Xue, H.G. Othmer, R. Erban, *From Individual to Collective Behavior of Unicellular Organisms: Recent Results and Open Problems*, vol. 1167 (AIP, Melville, NY, 2009), pp. 3–14
106. C. Xue, H.J. Hwang, K.J. Painter, R. Erban, Travelling waves in hyperbolic chemotaxis equations. Bull. Math. Biol. **73**(8), 1695–1733 (2011)
107. C. Xue, E.O. Budrene, H.G. Othmer, Radial and spiral stream formation in proteus mirabilis colonies. PLoS Comput. Biol. **7**(12), e1002332 (2011)